

Multivariate Medians for Image and Shape Analysis

Martin Welk

Institute of Biomedical Image Analysis
UMIT TIROL – Private University for Health Sciences,
Biomedical Informatics and Technology
Eduard-Wallnöfer-Zentrum 1, 6060 Hall/Tyrol, Austria
martin.welk@umit-tirol.at

June 25, 2021

Abstract

Having been studied since long by statisticians, multivariate median concepts found their way into the image processing literature in the course of the last decades, being used to construct robust and efficient denoising filters for multivariate images such as colour images but also matrix-valued images. Based on the similarities between image and geometric data as results of the sampling of continuous physical quantities, it can be expected that the understanding of multivariate median filters for images provides a starting point for the development of shape processing techniques. This paper presents an overview of multivariate median concepts relevant for image and shape processing. It focusses on their mathematical principles and discusses important properties especially in the context of image processing.

1 Introduction

For almost half a century, the median filter has established itself as an efficient tool for filtering of univariate signals and images [69]. Despite its simplicity, it has favourable properties as a denoising method. Whereas average filters and their variants such as Gaussian smoothing are useful for denoising e.g. additive Gaussian noise, they break down in the presence of noise featuring more outliers such as impulsive noise. In contrast, the median filter performs surprisingly well in removing such noise; at the same time, it is capable of preserving sharp signal or image boundaries. Moreover, an interesting connection to partial differential equations (PDEs) could be proven [27].

The success of univariate median filtering has inspired researchers to investigate similar procedures for multivariate images. In several works on this subject [5, 67, 84], the minimisation of an objective function composed of distances of the median point to the input values was considered, building on or partly rediscovering concepts that had been around long before in the statistical community [25] and are nowadays often referred to as L^1 medians. In the statistical literature, however, shortcomings of this concept have been discussed since the 1940s [28], and various alternative ideas have been developed since then [66]. Recently, attempts have been made to introduce some of these alternative concepts to image processing [78, 82].

The ability of the median to reduce a data set to a single value representing its position, and doing so in a way that is hardly sensitive to outliers in the data, makes multivariate medians also an interesting candidate for the analysis of geometric data such as point clouds in the real affine space, or more generally on manifolds. Resulting from the sampling of continuous-scale physical quantities, such geometric data are not far from image data, and image analysis techniques have been adapted successfully for their processing, see [19] for an example, or [20] for combined processing of shape and image data in the case of textured surfaces. Although few references to median filtering of geometric data can be found in the literature so far – see e.g. [66, Sec. 7] for a short discussion of medians for points on a sphere –, it can therefore be expected that a thorough understanding of multivariate median filtering of images can serve as a starting point for robust shape processing techniques.

This paper aims at giving an overview of multivariate median concepts that can be useful for processing images and shapes. In the course of the paper, the underlying mathematical structures and principles are presented, and linked to resulting properties of the filters that are particularly relevant for the processing of image and shape data. Results on connections between multivariate median filters and PDE-based image filters are reviewed. Results from existing work, including some by the author of this paper, are reported. In order to present the overarching principles and ideas, proofs of individual results are generally omitted, although hints at important ideas behind these proofs are given where appropriate.

The remainder of this paper is organised as follows. In Section 2, different ways to define univariate medians for discrete sets and continuous distributions are juxtaposed, and some equivariance properties and algorithmic aspects are reviewed. Median filtering of univariate (grey-scale) images is discussed in Section 3, covering also a space-continuous model and its relation to PDEs as well as an extension to adaptive neighbourhoods (so-called morphological amoebas). In Section 4, a selection of multivariate median concepts are presented, namely, the L^1 median, Oja’s simplex median, a transformation–retransformation L^1 median, the half-space median and the convex-hull-stripping median. It will be shown how these concepts are derived from generalising different variants of univariate median definitions. Properties of multivariate median concepts that are relevant to image and shape processing are pointed out, with emphasis on the relation between discrete and continuous models, and equivariance properties. Remarks on algorithmic aspects are included. The short Section 5 points out some specific aspects of median filtering of multivariate images, focussing on the proper handling of different dimensionality of image domains and data ranges. Section 6 gives an overview of the results on approximations of PDEs by multivariate median filters that have been achieved so far, including one result the proof of which is still awaiting (and which is stated as conjecture therefore). The paper ends with a short summary in Section 7.

Notations. Let us briefly introduce a few notations that will be used throughout this paper. By \mathbb{R} we denote the set of real numbers. The symbol \mathbb{R}^+ stands for positive real numbers whereas \mathbb{R}_0^+ names nonnegative real numbers. As usual, \mathbb{R}^n is the n -dimensional real vector or affine space which will sometimes be equipped with the standard Euclidean structure. In this case, $\|\mathbf{v}\|$ is the Euclidean norm of a vector $\mathbf{v} \in \mathbb{R}^n$, and $\langle \mathbf{v}, \mathbf{w} \rangle$ the scalar product of vectors $\mathbf{v}, \mathbf{w} \in \mathbb{R}^n$. By \mathbb{Z} we denote the set of integers.

A *multiset* is a set with (integer) multiplicities; standard notations for sets, including union and intersection, are used for multisets in an intuitive way. The cardinality of a set or multiset S will be written as $\#S$. The convex hull of a set or multiset $S \subset \mathbb{R}^n$ will be denoted by $[S]$, where $[x_1, \dots, x_n]$ abbreviates $\{x_1, \dots, x_n\}$ for finite multisets. The volume (n -dimensional

measure) of a measurable point set $S \subset \mathbb{R}^n$ will be written as $|S|$. In particular, $||S||$ is the volume of the convex hull of S .

The concatenation of functions g and f will be denoted by $f \circ g$, i.e. $(f \circ g)(x) := f(g(x))$. At some points, reference will be made to distributions over \mathbb{R} or \mathbb{R}^n ; their spaces will be denoted by $\mathcal{D}'(\mathbb{R})$ or $\mathcal{D}'(\mathbb{R}^n)$, respectively, compare [74, 75].

For error estimates as well as for algorithmic complexity statements, we will use the common \mathcal{O} Landau notation. Just recall that for error estimates, $\mathcal{O}(f(\varepsilon))$ denotes the set of functions $g(\varepsilon)$ which for $\varepsilon \rightarrow 0$ are bounded by a constant multiple of $f(\varepsilon)$, whereas for complexity statements $\mathcal{O}(f(N))$ denotes the set of functions $g(N)$ which are bounded by constant multiples of $f(N)$ for $N \rightarrow \infty$.

2 Univariate Median

In this section, we collect basic facts about the median of real-valued data in various settings, ranging from finite multisets via countable weighted sets up to continuous densities over \mathbb{R} .

Whereas practical computations always act on finite, thus discrete, data, the continuous case is important for a proper theoretical foundation of the intended application of medians in image and shape analysis since we always understand discrete images and shapes as samples of space-continuous objects.

We put special emphasis on characterisations of the median by minimisation properties as these play a central role for the later generalisation to the multivariate case.

2.1 Median for Unweighted Discrete Data

Rank-order definition. The most basic concept of the median relies on rank order, taking the middle element of an ordered sequence.

DEFINITION 1 (Median by rank-order). Let a finite multiset $\mathcal{X} = \{x_1, \dots, x_N\}$ of real numbers $x_1, \dots, x_N \in \mathbb{R}$ be given. Assume that the elements of \mathcal{X} are arranged in ascending order, $x_1 \leq \dots \leq x_N$. If N is odd, the *median* of \mathcal{X} is given by $x_{(N+1)/2}$. If N is even, the median is given by the interval $[x_{N/2}, x_{N/2+1}]$.

In the case of even N , there is an ambiguity; one could define either of the two values in the middle or e.g. their arithmetic mean as the median of \mathcal{X} . As this ambiguity does not play a central role in the context of this work, we will prefer the set-valued interpretation as stated in the Definition and not further elaborate on disambiguation strategies. We will still colloquially speak of “the” median even in this case.

An extrema-stripping procedure to determine the median. An (albeit inefficient) way to determine the median of a multiset can be based directly on this rank-order definition:

DEFINITION 2 (Median by extrema-stripping). Let a finite multiset \mathcal{X} of real numbers be given. Delete its smallest and greatest element, then again the remaining smallest and greatest element etc., until an empty set is obtained. The one or two points that were deleted in the very last step of this sequence are medians, with the entire median set given as their convex hull.

The median as 1/2-quantile. The median is also the 1/2-quantile of the given set, i.e. the smallest number μ for which at least half of the given data are less or equal μ . In the following definition, $\#S$ denotes the cardinality of a finite multiset S .

DEFINITION 3 (Median as 1/2-quantile). Let \mathcal{X} be a finite multiset of real numbers. The median of \mathcal{X} is defined as

$$\text{med}(\mathcal{X}) := \min \{ \mu \in \mathbb{R} \mid \#(\mathcal{X} \cap (-\infty, \mu]) \geq \frac{1}{2} \# \mathcal{X} \} . \quad (1)$$

Note that the ambiguity in the case of even $\# \mathcal{X} = N$ is resolved here by taking the minimum. A more symmetric definition again implies a set-valued median.

DEFINITION 4 (Median as 1/2-quantile, symmetric). Let \mathcal{X} be a finite multiset of real numbers. The median of \mathcal{X} is defined as

$$\begin{aligned} \text{med}(\mathcal{X}) := & \{ \mu \in \mathbb{R} \mid \#(\mathcal{X} \cap (-\infty, \mu]) \geq \frac{1}{2} \# \mathcal{X} \} \\ & \cap \{ \mu \in \mathbb{R} \mid \#(\mathcal{X} \cap [\mu, +\infty)) \geq \frac{1}{2} \# \mathcal{X} \} . \end{aligned} \quad (2)$$

The median as point of maximal half-line depth. The latter characterisation can be rephrased by defining the median as the set of points which split the data multiset as symmetric as possible. This characterisation of the median goes back to the work by Hotelling [31] and has been picked up by Tukey [70].

DEFINITION 5 (Median as point of maximal half-line depth). For a finite multiset \mathcal{X} of real numbers, define the median of \mathcal{X} as

$$\text{med}(\mathcal{X}) := \underset{\mu \in \mathbb{R}}{\text{argmax}} \min \{ \#(\mathcal{X} \cap (-\infty, \mu]), \#(\mathcal{X} \cap [\mu, +\infty)) \} . \quad (3)$$

The count $\min \{ \#(\mathcal{X} \cap (-\infty, \mu]), \#(\mathcal{X} \cap [\mu, +\infty)) \}$ that indicates for any μ the number of data points that are contained at least in a half-line starting at μ , is called *half-line depth* of μ w.r.t. \mathcal{X} .

Note that in a finite set (without multiplicities) the half-line depth of a data point is simply its rank or reverse rank. The extrema-stripping procedure from Definition 2 then actually enumerates the data points in the order of increasing half-line depth; the half-line depth of each data point is the ordinal number of the step in which it is deleted.

The median as minimiser of a convex function. As has been observed first by Jackson [32], the median of real numbers can also be defined via an optimisation property.

DEFINITION 6 (Median as minimiser). Let $\mathcal{X} = \{x_1, \dots, x_N\}$ be a multiset of real numbers $x_1, \dots, x_N \in \mathbb{R}$. The median of \mathcal{X} is

$$\text{med}(\mathcal{X}) := \underset{\mu \in \mathbb{R}}{\text{argmin}} E_{\mathcal{X}}(\mu) , \quad E_{\mathcal{X}}(\mu) := \sum_{i=1}^N |\mu - x_i| . \quad (4)$$

In this formulation, the order of real numbers is not explicitly invoked. The objective function $E_{\mathcal{X}}(\mu)$ is a continuous, piecewise linear function with a kink at every data value $\mu = x_i$. For even N , there will be a constant segment over the interval formed by the two middle values in the rank order.

2.2 Median for Weighted Discrete Data

The median concept can easily be extended to weighted data. We assume that \mathcal{X} is a countable set of real numbers, on which a positive weight function $w : \mathcal{X} \rightarrow \mathbb{R}^+$ is given. We will require w to have unit total weight, i.e. $\sum_{x \in \mathcal{X}} w(x) = 1$.

Quantile-based definition. We can define the median of weighted data analogously to (1) or (2).

DEFINITION 7 (Weighted median as 1/2-quantile). Let \mathcal{X} be a countable set of real numbers with a positive weight function $w : \mathcal{X} \rightarrow \mathbb{R}^+$ of unit total weight. The median of the weighted set \mathcal{X} is

$$\text{med}(\mathcal{X}, w) := \min \left\{ \mu \in \mathbb{R} \mid \sum_{x \in \mathcal{X}, x \leq \mu} w(x) \geq \frac{1}{2} \right\}. \quad (5)$$

DEFINITION 8 (Weighted median as 1/2-quantile, symmetric). Let \mathcal{X}, w be as in Definition 7. The median of the weighted set \mathcal{X} is

$$\begin{aligned} \text{med}(\mathcal{X}, w) := & \left\{ \mu \in \mathbb{R} \mid \sum_{x \in \mathcal{X}, x \leq \mu} w(x) \geq \frac{1}{2} \right\} \\ & \cap \left\{ \mu \in \mathbb{R} \mid \sum_{x \in \mathcal{X}, x \geq \mu} w(x) \geq \frac{1}{2} \right\}. \end{aligned} \quad (6)$$

Weighted half-line depth. The half-line depth definition of the median can be translated as follows.

DEFINITION 9 (Weighted median as point of maximal half-line depth). Let \mathcal{X}, w be as in Definition 7. The median of the weighted set \mathcal{X} is

$$\text{med}(\mathcal{X}, w) := \operatorname{argmax}_{\mu \in \mathbb{R}} \min \left\{ \sum_{x \in \mathcal{X}, x \leq \mu} w(x), \sum_{x \in \mathcal{X}, x \geq \mu} w(x) \right\}. \quad (7)$$

For $\mu \in \mathbb{R}$, we call $\min \left\{ \sum_{x \in \mathcal{X}, x \leq \mu} w(x), \sum_{x \in \mathcal{X}, x \geq \mu} w(x) \right\}$ *half-line depth* of μ w.r.t. (\mathcal{X}, w) .

If \mathcal{X} is finite, adapting the extrema-stripping procedure to weighted medians is possible with proper bookkeeping of the weighted half-line depth of points during the deletion process; in each step, one deletes the extremum point (minimum or maximum) with lesser half-line depth, or both simultaneously if their half-line depths are equal.

Minimisation property. The minimisation definition (4), too, can easily be adapted to weighted data.

DEFINITION 10 (Weighted median as minimiser). Let \mathcal{X}, w be as in Definition 7. The median of the weighted set \mathcal{X} is

$$\text{med}(\mathcal{X}, w) := \operatorname{argmin}_{\mu \in \mathbb{R}} E_{\mathcal{X}, w}(\mu), \quad E_{\mathcal{X}, w}(\mu) := \sum_{x \in \mathcal{X}} w(x) |\mu - x|. \quad (8)$$

2.3 Median of Continuous Data

The various definitions of the median for weighted sets can easily be generalised to continuous data described by densities.

DEFINITION 11 (Normalised regular density on \mathbb{R}). Let $\gamma : \mathbb{R} \rightarrow \mathbb{R}_0^+$ be a nonnegative integrable function with unit total weight $\int_{\mathbb{R}} \gamma(x) dx = 1$. Then γ is called *normalised regular density* on \mathbb{R} .

Quantile-based definition. We start again by definitions of the median as a 1/2-quantile, see [28] where the so-defined median is called *arithmetic median*.

DEFINITION 12 (Continuous median as 1/2-quantile). The median of a normalised regular density γ is defined as

$$\text{med}(\gamma) := \min \left\{ \mu \in \mathbb{R} \mid \int_{-\infty}^{\mu} \gamma(x) dx \geq \frac{1}{2} \right\}, \quad (9)$$

DEFINITION 13 (Continuous median as 1/2-quantile, symmetric). The median of a normalised regular density γ is defined as

$$\begin{aligned} \text{med}(\gamma) := & \left\{ \mu \in \mathbb{R} \mid \int_{-\infty}^{\mu} \gamma(x) dx \geq \frac{1}{2} \right\} \\ & \cap \left\{ \mu \in \mathbb{R} \mid \int_{\mu}^{+\infty} \gamma(x) dx \geq \frac{1}{2} \right\}. \end{aligned} \quad (10)$$

For regular densities as specified so far, the inequalities $\int \gamma dx \geq 1/2$ will even be fulfilled with equality. However, (9) and (10) can even be used verbatim for a more general class of distribution-valued densities $\gamma \in \mathcal{D}'(\mathbb{R})$ that can be decomposed into a regular (real-valued) density $\{\gamma\}$ with a countable sum of weighted delta (Dirac) peaks, thus representing the combination of a continuous distribution of values (in which each particular number has negligible weight) with a weighted discrete set as in (5), (6). In this case the inequalities $\int \gamma dx \geq 1/2$ may not be satisfied with equality if the median happens to be at a delta peak of γ .

Continuous half-line depth. The characterisation (10) can again be rewritten in a half-line depth form, where the continuous half-line depth is determined by integrals.

DEFINITION 14 (Continuous median as point of maximal half-line depth). For a normalised regular density γ , its median is defined as

$$\text{med}(\gamma) := \operatorname{argmax}_{\mu \in \mathbb{R}} \min \left\{ \int_{-\infty}^{\mu} \gamma(x) dx, \int_{\mu}^{+\infty} \gamma(x) dx \right\}. \quad (11)$$

Continuous extrema stripping. Even an extrema-stripping formulation of the continuous median is possible. To this end, the stripping procedure must be stated as a time-continuous process. We will give this definition for simplicity in the case of a density with a connected compact support set.

DEFINITION 15 (Continuous median by extrema-stripping). Let γ be a normalised regular density which is zero outside some interval $[a_0, b_0]$ and nonzero in its interior (a_0, b_0) . Consider then the ordinary differential equations

$$a'(t) = (\gamma(a(t)))^{-1}, \quad b'(t) = -(\gamma(b(t)))^{-1} \quad (12)$$

with the initial conditions

$$a(0) = a_0 , \quad b(0) = b_0 . \quad (13)$$

This initial boundary value problem yields a monotonically increasing $a : [0, T] \rightarrow \mathbb{R}$ and monotonically decreasing $b : [0, T] \rightarrow \mathbb{R}$ on an interval $[0, T]$ where T is chosen such that $a(T) = b(T)$, and the median of γ is defined as

$$\text{med}(\gamma) := a(T) . \quad (14)$$

For each $t \in [0, T]$, we call t the continuous half-line depth of $a(t)$ and $b(t)$.

Minimisation property. Provided that γ is compactly supported, a reformulation using a minimisation property is again possible. This median is called *geometric median* in [28].

DEFINITION 16 (Continuous median as minimiser). Let γ be a normalised regular density with compact support. The median of γ is

$$\text{med}(\gamma) := \underset{\mu \in \mathbb{R}}{\text{argmin}} E_\gamma(\mu) , \quad E_\gamma(\mu) := \int_{\mathbb{R}} \gamma(x) |\mu - x| dx . \quad (15)$$

The requirement of compact support of γ can be replaced by a weaker condition that ensures that the integral in E_γ converges.

Non-uniqueness of the median is much less of a problem here than in the case of discrete data as it occurs only if the support of γ is contained in two separate intervals each of which contains exactly half the total weight of γ . In particular, if the support of γ is an interval, and γ has only isolated zeros within this interval, the median is unique.

2.4 Equivariance Properties

As the median in the sense of (1), (5) or (2), (6) depends on nothing but the total order of the data, it can be generalised to data in any totally ordered set R instead of \mathbb{R} . Moreover, the median is equivariant w.r.t. any strictly monotonically increasing map $T : R \rightarrow R$, i.e.

$$T(\text{med}(\mathcal{X})) = \text{med}(T(\mathcal{X})) \quad (16)$$

where

$$T(\mathcal{X}) := \{T(x) \mid x \in \mathcal{X}\} \quad (17)$$

denotes element-wise application of T to all members of \mathcal{X} (retaining their cardinalities), and similarly

$$T(\text{med}(\mathcal{X}, w)) = \text{med}(T(\mathcal{X}, w \circ T^{-1})) . \quad (18)$$

Note that the weight function w needs to be adapted using the inverse map T^{-1} which obviously exists.

Specifically for $R = \mathbb{R}$ we notice that the symmetric definitions (2), (6) are also equivariant under strictly monotonically decreasing maps T .

For the median of continuous densities (9) or (10) over \mathbb{R} the equivariance w.r.t. strictly monotone transformations T is given by

$$T(\text{med}(\gamma)) = \text{med}(\gamma^T) . \quad (19)$$

where γ^T is given as

$$\gamma^T(x) := \frac{d}{dy} \left(\int_{-\infty}^{T^{-1}(y)} \gamma(z) dz \right) (x) , \quad (20)$$

i.e. the uniquely determined density for which

$$\int_{-\infty}^{T(x)} \gamma^T(y) dy = \int_{-\infty}^x \gamma(y) dy \quad \text{for all } x \in \mathbb{R} . \quad (21)$$

In the case of (10), the equivariance property (19) again holds for strictly monotonically decreasing maps T , too.

2.5 Algorithmic Aspects

In the processing of images by median filtering, see Section 3, median computations will have to be carried out multiple times. Efficient algorithms are therefore relevant for the practicability of such filters.

Unweighted median. Finding the median of a finite multiset \mathcal{X} of size N is what is known in algorithmics as a *selection problem*. Whereas in principle one could sort the data in \mathcal{X} based on their total order (for which several algorithms with $\mathcal{O}(N \log N)$ computational complexity exist), the selection problem does actually not require the complete order of the data, and can be solved even by $\mathcal{O}(N)$ operations. A popular selection algorithm is Quick-Select which has $\mathcal{O}(N)$ average complexity but $\mathcal{O}(N^2)$ worst-case complexity. By using the *median of medians* procedure [12] for selecting the so-called *pivot* element in Quick-Select, its worst-case complexity can be improved to $\mathcal{O}(N)$.

Weighted median. The median of a finite set \mathcal{X} with weights $w : \mathcal{X} \rightarrow \mathbb{R}^+$ can be computed by sorting \mathcal{X} , which takes $\mathcal{O}(N \log N)$ operations, followed by cumulating the weights for the members of \mathcal{X} in ascending order, which requires $\mathcal{O}(N)$ effort, yielding an overall $\mathcal{O}(N \log N)$ complexity, both worst-case and average. In [52] an algorithm with $\mathcal{O}(N)$ average complexity is proposed.

3 Univariate Median Filtering of Images

The definition of median filters for grey-value images and some important properties of these are discussed in this section.

3.1 Standard Discrete Median Filtering

A discrete grey-value image u is an array of intensities $u_{i,j}$ where $i = 1, \dots, N_x$ and $j = 1, \dots, N_y$ enumerate the locations (pixels) of a regular grid in horizontal and vertical direction, respectively.

The classical median filter [69] processes a discrete grey-value image u using a *sliding window*. A sliding window can be described by a set $S = \{(\Delta i_1, \Delta j_1), \dots, (\Delta i_r, \Delta j_r)\}$ of integer pairs $(\Delta i_k, \Delta j_k)$; typically $(0, 0)$ is one of these pairs, and the others are centered around $(0, 0)$, often in a symmetric way. For example, a $(2\ell + 1) \times (2\ell + 1)$ window is given by $S = \{-\ell, \dots, +\ell\} \times \{-\ell, \dots, +\ell\}$, or an approximately disc-shaped window of radius r by $S = \{(\Delta i, \Delta j) \mid i, j \in \mathbb{Z}, i^2 + j^2 \leq r^2\}$.

For each pixel (i, j) , the sliding window is shifted to this pixel to select a set of pixels around (i, j) and generate new (filtered) pixel values from the selected pixels. Using the notation $(i, j) + S := \{(i + \Delta i, j + \Delta j) \mid (\Delta i, \Delta j) \in S\}$, the median filter assigns the median of all $u_{i', j'}$ for $(i', j') \in (i, j) + S$ to pixel (i, j) in the median-filtered image v ,

$$v_{i,j} := \text{med}\{u_{i',j'} \mid (i', j') \in (i, j) + S\}. \quad (22)$$

For pixels near the boundary where $(i, j) + S$ contains locations outside the image domain $\{1, \dots, N_x\} \times \{1, \dots, N_y\}$, a suitable boundary treatment needs to be defined, which we do not discuss further here.

It is important to notice that the filter consists of two steps: the *selection step* that extracts values from the input image using the sliding window, and the *aggregation step* that uses the median to generate the new value from the extracted values. This is the universal structure of local image filters; the specification of selection and aggregation step defines the particular filter.

The entire process can be iterated by applying the median filter to the median-filtered image, and so on. This is called *iterative median filtering*.

Properties. The median is known as a robust position measure [69] in statistics, and bequeathes its robustness to the median filter for images. In particular, the median filter is known for its denoising capabilities even in the presence of some sorts of non-Gaussian (heavy-tailed) noise like salt-and-pepper or uniform impulse noise. At the same time, it can preserve sharp edges, since for pixels near an edge, the sliding window contains some pixels from either side of the edge, and the median will be on the side of the majority, thus yielding an intensity clearly belonging to one side, and not creating intermediate values.

When iterating median filtering, several phenomena are observed. On one hand, small image structures are eliminated. Whereas filtered images still show sharp edges, corners are progressively rounded.

On the other hand, non-trivial stationary patterns can appear during the iterated filtering process, most prominent with small sliding windows such as 3×3 or 5×5 , but not limited to these. These so-called *root signals* have been studied e.g. by Eckhardt [23]. The existence of such patterns is inherent to the discrete median filtering process, whereas their actual occurrence depends on the interaction between small-scale image structures and sliding windows, and can be considered as filtering artifacts related to the resolution limit of the discrete image. Worst-case examples are a checkerboard pattern (say, all pixels (i, j) with $i + j$ even are black, and all others white) which is stationary under whatever $(2\ell + 1) \times (2\ell + 1)$ median filter, and a stripe pattern (say, all pixels (i, j) with i even are black, and all others white) which is inverted in each iteration.

3.2 Space-Continuous Median Filtering

Whereas practical image processing always has to deal with discrete images, a continuous viewpoint is helpful for the theoretical understanding of image processing. Image acquisition creates discrete images by sampling spatially continuous physical quantities, and involves the choice of a sampling grid, which is, in essence, arbitrary. For image processing methods to be meaningful, they need to be consistent with a continuous reality, and depend as little as possible on sampling.

To support theoretical analysis of median filtering, it is therefore of interest to consider a median filtering process for space-continuous images. Thus, we interpret a (planar) grey-value image as a bounded function from a suitable function space over a region of \mathbb{R}^2 , which should be compact and connected. For a deeper analysis, several function spaces have been proposed, such as functions of bounded variation (BV) or sums of the BV space (to represent piecewise smooth images) and Sobolev spaces (to represent noise and/or texture components), see e.g. [7, 6, 48, 86] and the numerous references therein. In this work, we will for simplicity assume that images are smooth functions.

DEFINITION 17 (Smooth image). Let $\Omega \subset \mathbb{R}^2$ be compact and equal to the closure of its interior. Let $u : \Omega \rightarrow \mathbb{R}$ be a bounded smooth function on Ω . We call u *smooth image with domain Ω* .

We denote by ∇u the gradient of u , and by D^2u its Hessian, i.e. the symmetric 2×2 -tensor of its second-order derivatives. We call $\mathbf{x} \in \Omega$ *regular point of u* if $\nabla u(\mathbf{x}) \neq \mathbf{0}$.

We will now give some definitions to formalise the two steps of a local filter in a space-continuous setting. We start with the selection step.

DEFINITION 18 (Selector). Let u be a smooth image with domain $\Omega \subset \mathbb{R}^2$. Let S be a map that assigns to each location $\mathbf{x} \in \Omega$ a closed neighbourhood $S(\mathbf{x}) \subset \mathbb{R}^2$. Then S is called *selector for u* .

Whereas Definition 18 actually allows some more generality (with regard to the subsequent section), the continuous median filter discussed in this section will strictly follow the sliding-window idea by deriving all $S(\mathbf{x})$ from just one set S_0 by shifting, $S(\mathbf{x}) = \mathbf{x} + S_0 := \{\mathbf{x} + \mathbf{y} \in \mathbb{R}^2 \mid \mathbf{y} \in S_0\}$.

Varying the size of the neighbourhood for filtering will be an important step in the theoretical analysis, thus we specify such a procedure by a further definition.

DEFINITION 19 (Scaled selector). Let Σ be a map that assigns to any smooth image u and any positive ϱ a selector $\Sigma_{u,\varrho}$ for u . Assume that for each u and each location \mathbf{x} and for all $\varrho < \sigma$ the inclusion $\Sigma_{u,\varrho}(\mathbf{x}) \subset \Sigma_{u,\sigma}(\mathbf{x})$ holds, and $\bigcap_{\varrho>0} \Sigma_{u,\varrho}(\mathbf{x}) = \{\mathbf{x}\}$. Then Σ is called *scaled selector for u* .

Our main example of a scaled selector in this section will be the family $\mathcal{D} = \{D_\varrho \mid \varrho > 0\}$ of discs with radius ϱ given by $D_\varrho(\mathbf{x}) = \{\mathbf{y} \in \mathbb{R}^2 \mid \|\mathbf{y} - \mathbf{x}\| \leq \varrho\}$.

Let us now turn to the second step of a local filter, aggregation.

DEFINITION 20 (Aggregator). Let Γ be a family of integrable densities $\gamma : \mathbb{R} \rightarrow \mathbb{R}_0^+$. Let A be a functional that maps densities $\gamma \in \Gamma$ to values $A(\gamma) \in \mathbb{R}$. Then A is called a *Γ -aggregator on \mathbb{R}* .

In particular, the space-continuous median is an aggregator, where Γ can be either the regular densities mainly considered in Section 2.3 or the distributions $\mathcal{D}'(\mathbb{R})$. Both steps are combined in the following definition.

DEFINITION 21 (Local filters). Let u be a smooth image with domain Ω , and S a selector for u .

For each $\mathbf{x} \in \Omega$, let $u|S(\mathbf{x})$ be the restriction of u to $\Omega \cap S(\mathbf{x})$, i.e. $u|S(\mathbf{x}) : \Omega \cap S(\mathbf{x}) \rightarrow \mathbb{R}$, $(u|S(\mathbf{x}))(\mathbf{y}) = u(\mathbf{y})$ for $\mathbf{y} \in \Omega \cap S(\mathbf{x})$.

Let A be a Γ -aggregator on \mathbb{R} . If for each $\mathbf{x} \in \Omega$, the density $\gamma(u|S(\mathbf{x})) : \mathbb{R} \rightarrow \mathbb{R}_0^+$ of the values of $u|S(\mathbf{x})$ belongs to Γ , we define $A(u, S) : \Omega \rightarrow \mathbb{R}$ by $A(u, S)(\mathbf{x}) := A(\gamma(u|S(\mathbf{x})))$ for all $\mathbf{x} \in \Omega$ and call it (A, S) -filtering of u .

If Σ is a scaled selector for u , and the $(A, \Sigma_{u, \varrho})$ -filtering of u exists for all $\varrho > 0$, we call the family of $(A, \Sigma_{u, \varrho})$ -filterings the (A, Σ) -filtering of u .

Continuous median filtering can then be described as (med, S) -filtering with a suitable selector. For example, one step of (med, D_ϱ) -filtering assigns to each location \mathbf{x} as filtered value the median of the grey-value density within a disc of radius ϱ around this location.

In the following we will be interested in the family of such filters, i.e. the (scaled) $(\text{med}, \mathcal{D})$ -filtering.

3.3 Infinitesimal Analysis of Median Filtering

When the neighbourhood radius ϱ of a (med, D_ϱ) -filtering is reduced, the filtering result $\text{med}(u, D_\varrho)$ will differ less and less from u itself. However, in iterated filtering the reduced filtering effect of a single step can be compensated by increasing the number of iterations by a suitable scale. In the limit $\varrho \rightarrow 0$, the number of filtering steps goes to infinity whereas the effect of each step goes to zero. Instead of a sequence of progressively filtered images, an image evolution with a continuous time parameter results.

DEFINITION 22 (Image evolution). Let $\Omega \subset \mathbb{R}^2$ be as in Definition 17, and $[0, T] \subset \mathbb{R}$ an interval. The coordinates of Ω will be called *spatial coordinates*, the additional coordinate from $[0, T]$ *time coordinate*. Let $u : \Omega \times [0, T] \rightarrow \mathbb{R}$ be a bounded smooth function. We call u an *image evolution with spatial domain Ω* .

We denote by ∇u the spatial gradient of u , i.e. the vector of its first-order derivatives w.r.t. the spatial coordinates, and by D^2u its spatial Hessian, i.e. the 2×2 -tensor of its second-order derivatives w.r.t. the spatial coordinates.

By $u(t^*)$ for $t^* \in [0, T]$ we denote the smooth image with $u(t^*)(\mathbf{x}) := u(\mathbf{x}, t^*)$ for all $\mathbf{x} \in \Omega$.

Time-continuous image evolutions can be described by partial differential equations (PDEs). To capture the limit transition $\varrho \rightarrow 0$ of an iterated local filter, including the appropriate scaling of the iteration count, we use the following definition.

DEFINITION 23 (Regular PDE limit). Let Σ be a scaled selector in \mathbb{R}^2 , and A a Γ -aggregator on \mathbb{R} .

The second-order PDE $u_t = F(\nabla u, D^2u)$ is the *regular PDE limit of (A, Σ) -filtering with time scale $\tau(\varrho)$* if for each smooth image u the (A, Σ) -filtering exists, and if there

exists an $\varepsilon > 0$ such that for each regular point \mathbf{x} of u one has for $\varrho \rightarrow 0$

$$\frac{A(u, \Sigma_{u, \varrho})(\mathbf{x}) - u(\mathbf{x})}{\tau(\varrho)} - F(\nabla u(\mathbf{x}), D^2 u(\mathbf{x})) = \mathcal{O}(\varrho^\varepsilon). \quad (23)$$

PDE limit of median filtering. Guichard and Morel [27] proved that space-continuous median filtering approximates for $\varrho \rightarrow 0$ a well-known image filtering PDE evolution, namely *(mean) curvature flow* [4].

With our definitions above, we can state their result as follows.

PROPOSITION 1 [27]. *For a smooth image, $(\text{med}, \mathcal{D})$ -filtering with the median as aggregator and the family of discs \mathcal{D} as scaled selector has the regular PDE limit with time scale $\tau(\varrho) = \varrho^2/6$ given by*

$$u_t = \|\nabla u\| \operatorname{div} \left(\frac{\nabla u}{\|\nabla u\|} \right). \quad (24)$$

The PDE (24) can be written in various forms. We mention that $\operatorname{div}(\nabla u / \|\nabla u\|)$ gives at any regular image location \mathbf{x} the curvature $\kappa(\mathbf{x})$ of the level line passing through \mathbf{x} . Therefore (24) can be written as [60, (2.25)]

$$u_t = \kappa \|\nabla u\|. \quad (25)$$

Moreover, if ξ denotes at each image location a unit vector perpendicular to the gradient, thus, in the direction of the local level line, one can write the same equation as [60, (2.26)]

$$u_t = u_{\xi\xi}, \quad (26)$$

i.e. a diffusion process in level line direction, which gives reason to the names *geometric diffusion* or *geometric heat flow* that are also often used.

As an application of the result in Proposition 1, it has been proposed that median filtering may be used as a discretisation of mean curvature flow, see e.g. [42] which anticipated the relation between the two processes, and [33].

3.4 Combination with Adaptive Structuring Elements

An interesting modification of median filtering is obtained by altering the selection step to use image-adaptive neighbourhoods. Instead of a sliding window that is shifted to each pixel, the window shape is determined at each pixel individually. One approach to do this are the *morphological amoebas* introduced by Lerallut et al. [38, 39]. Here, the distance between neighbouring pixels is measured by an *amoeba distance* combining standard Euclidean distance with contrast information, i.e.

$$d_\beta((i, j), (i', j')) := 1 + \beta |u_{i,j} - u_{i',j'}| \quad (27)$$

for two pixels (i, j) and (i', j') in the image u which are either horizontal or vertical neighbours, i.e. $|i - i'| + |j - j'| \leq 1$. This distance measure is extended to non-adjacent pixels via shortest paths, and for each pixel (i, j) the amoeba $A_{\beta, \varrho}(i, j)$ of radius ϱ is defined as the set of all pixels the amoeba distance of which to (i, j) does not exceed ϱ .

An amoeba median filter is then obtained by

$$v_{i,j} := \text{med}\{u_{i',j'} \mid (i', j') \in A_{\beta,\varrho}(i, j)\}. \quad (28)$$

Retaining this basic procedure, the amoeba distance (27) can be modified in several ways. Following [83], the 4-neighbourhoods in which the amoeba distance is defined first can be extended to 8-neighbourhoods for a better approximation of rotational invariance. Moreover, the L^1 summation of spatial Euclidean distance and contrast can be replaced with a Euclidean summation. Combining these changes, one has [83]

$$d_\beta((i, j), (i', j')) := \sqrt{(i - i')^2 + (j - j')^2 + \beta^2(u_{i,j} - u_{i',j'})^2} \quad (29)$$

for $|i - i'| \leq 1$, $|j - j'| \leq 1$, which is again extended to non-adjacent pixels via shortest paths.

Continuous amoeba median filtering. In [83], a space-continuous formulation of amoeba median filtering of planar grey-value images was proposed. Modelling the space-continuous selectors after (29), they are defined as

$$A_{\beta,\varrho}(\mathbf{x}) := \{\mathbf{x}' \in \mathbb{R}^2 \mid d_\beta(\mathbf{x}, \mathbf{x}') \leq \varrho\} \quad (30)$$

where the space-continuous amoeba metric d_β depends on the smooth image $u : \mathbb{R}^2 \supset \Omega \rightarrow \mathbb{R}$ and is given by

$$d_\beta(\mathbf{x}, \mathbf{x}') := \min_{\mathbf{c} : [0,1] \rightarrow \mathbb{R}^2} \int_0^1 \sqrt{\|\mathbf{c}'(s)\|^2 + \beta^2|(u \circ \mathbf{c})'(s)|^2} ds, \quad (31)$$

minimising over regular curves $\mathbf{c} : [0, 1] \rightarrow \mathbb{R}^2$ with $\mathbf{c}(0) = \mathbf{x}$, $\mathbf{c}(1) = \mathbf{x}'$. The metric d_β can immediately be interpreted as the distance on the Riemannian surface $\{(\mathbf{x}, \beta u(\mathbf{x})) \mid \mathbf{x} \in \Omega\} \subset \mathbb{R}^3$, i.e. the (vertically rescaled) *graph* of the function u .

If L^1 summation between the spatial distance and contrast is preferred, d_β may be defined instead as

$$d_\beta(\mathbf{x}, \mathbf{x}') := \min_{\mathbf{c} : [0,1] \rightarrow \mathbb{R}^2} \int_0^1 \|\mathbf{c}'(s)\| + \beta |(u \circ \mathbf{c})'(s)| ds \quad (32)$$

which corresponds to a different, Finslerian [9], metric on the image graph.

Obviously, the family $\mathcal{A}_{\beta,\varrho} := \{A_{\beta,\varrho}(\mathbf{x}) \mid \mathbf{x} \in \Omega\}$ is a selector, and $\mathcal{A}_\beta := \{\mathcal{A}_{\beta,\varrho} \mid \varrho > 0\}$ is a scaled selector for u in the sense of our definitions from Section 3.2.

PDE limit of continuous amoeba median filtering. In [83], the following result was proved which establishes a relation between amoebas as a space-adaptive modification of median filtering, and a space-adaptive modification which is fairly standard in the area of image filtering PDEs.

PROPOSITION 2 [83, Section 3.2]. *For a smooth image, $(\text{med}, \mathcal{A}_\beta)$ -filtering with the median as aggregator and the family of amoebas \mathcal{A}_β derived from the amoeba metric (31) as scaled selector has the regular PDE limit with time scale $\tau(\varrho) = \varrho^2/6$ given by*

$$u_t = \|\nabla u\| \operatorname{div} \left(g(\|\nabla u\|) \frac{\nabla u}{\|\nabla u\|} \right). \quad (33)$$

with the edge-detector function $g : \mathbb{R}_0^+ \rightarrow \mathbb{R}_0^+$ defined by

$$g(s) = \frac{1}{1 + \beta^2 s^2}. \quad (34)$$

The PDE (33) describes the *self-snakes* proposed in [59] as an image-sharpening evolution. It differs from (mean) curvature motion (24) just by inserting a decreasing edge-detector function g in the divergence expression. The specific function g from (34) coincides with one (the most popular one) of the diffusivity functions proposed for nonlinear isotropic diffusion by Perona and Malik [51], with the diffusivity parameter set to $1/\beta$. These functions were also proposed for use in the self-snakes equation in [59].

As shown further in [83], amoeba median filtering with the amoeba metric (32) instead of (31) yields the same PDE limit (33) but with a different edge-detector function g .

4 Multivariate Median Concepts

The simplicity of the univariate median and its properties as a robust position measure in data sets make it attractive to define similar concepts for multivariate (\mathbb{R}^n -valued) data. Research interest in this question can be traced back to Hayford’s 1902 work [29] where componentwise medians of geographical coordinates were used to find an approximate “center” of the population of the United States. However, componentwise application of the univariate median was recognised soon as dependent on the choice of coordinate systems, inducing the quest for proper multivariate concepts without such a dependency.

The first of these concepts was introduced in 1909 by Weber [76] in location theory; it was identified as a multivariate median in the 1920’s and introduced to the statistics literature [25] where it was followed by numerous papers over the subsequent decades (some of which rediscovered the concept) that considered theoretical properties [24, 26, 28, 43], efficient numerical concepts [8, 64, 72, 77], and applications [14]. Deficiencies of this concept, which is now known as L^1 median, caused the introduction of alternative multivariate median concepts since the 1970s [10, 15, 16, 30, 40, 44, 46, 47, 70]. For an overview see [66].

In the following we describe the L^1 median and some of the more recent concepts that will be used in the further course of this paper. With focus on their application for image and shape analysis we will pay specific attention to continuous formulations and equivariance properties.

4.1 L^1 Median

The L^1 median [76, 25] results from a straightforward generalisation of the minimisation property (4) of the univariate median in which absolute differences $|\mu - x_i|$ in \mathbb{R} are replaced by Euclidean distances $\|\mu - \mathbf{x}_i\|$ in \mathbb{R}^n .

Discrete data. We start again by the case of finite multisets describing discrete data.

DEFINITION 24 (Discrete L^1 median). Let a finite multiset $\mathcal{X} = \{\mathbf{x}_1, \dots, \mathbf{x}_N\}$ of data points $\mathbf{x}_i \in \mathbb{R}^n$ ($n \geq 2$) be given. The L^1 median $\text{med}_{L^1}(\mathcal{X})$ of \mathcal{X} is given by

$$\text{med}_{L^1}(\mathcal{X}) := \underset{\mu \in \mathbb{R}^n}{\text{argmin}} E_{\mathcal{X}}^{L^1}(\mu), \quad E_{\mathcal{X}}^{L^1}(\mu) := \sum_{i=1}^N \|\mu - \mathbf{x}_i\|. \quad (35)$$

The name L^1 median refers to the L^1 summation of the distances $\|\mu - \mathbf{x}_i\|$ in $E_{\mathcal{X}}^{L^1}(\mu)$.

Each of the individual distance functions $d_i(\mu) := \|\mu - \mathbf{x}_i\|$ is convex in \mathbb{R}^n but not strictly convex because it is linear along each ray starting from \mathbf{x}_i . As a consequence, if all data points

$\mathbf{x}_i \in \mathcal{X}$ are situated on one straight line in \mathbb{R}^n (an embedding of the affine space \mathbb{R} into \mathbb{R}^n), the L^1 median is equivalent to the univariate median on this line (via the embedding), and is therefore non-unique (set-valued) if n is even. In all other cases, the objective function $E_{\mathcal{X}}^{L^1}(\boldsymbol{\mu})$ is strictly convex since on each given straight line at least one of the d_i is strictly convex, and the L^1 median therefore unique. If all data points in \mathcal{X} are located on a hyperplane, their L^1 median obviously coincides with its $(n - 1)$ -dimensional counterpart.

Unlike in the univariate case where $E_{\mathcal{X}}(\boldsymbol{\mu})$ is always minimised by at least one of the given data points, the L^1 median will often be located somewhere inbetween, although in some generic cases the L^1 median still happens to be one of the given data points. For example, for four points in the plane that are corners of a convex quadrangle, their L^1 median is the intersection point of its diagonals; but if from four points in the plane one is located within the triangle defined by the others, this data point will be the L^1 median. Some simple point sets with their L^1 medians are depicted in Figure 1.

Variants of the L^1 median concept are obtained if the Euclidean norm $\|\cdot\|$ in the above definition is replaced by other norms in \mathbb{R}^n . With the L^1 (city-block) metric, it boils down to the componentwise median. Another possibility would be the L^∞ (maximum) norm. Dependent on the choice of the norm, such an L^1 median may be non-unique in more cases than with the Euclidean norm. We do not further discuss non-Euclidean L^1 medians here.

The generalisation of (35) to weighted countable sets is straightforward.

Continuous data. Similarly as in the univariate case, we formulate space-continuous versions of multivariate median definitions for normalised regular densities.

DEFINITION 25 (Normalised regular density on \mathbb{R}^n). Let $\gamma : \mathbb{R}^n \rightarrow \mathbb{R}_0^+$ be a compactly supported integrable function with unit total weight, $\int_{\mathbb{R}^n} \gamma(\mathbf{x}) \, d\mathbf{x} = 1$. Then γ is called *normalised regular density* on \mathbb{R}^n .

Generalising (15), we can define the L^1 median of such a density.

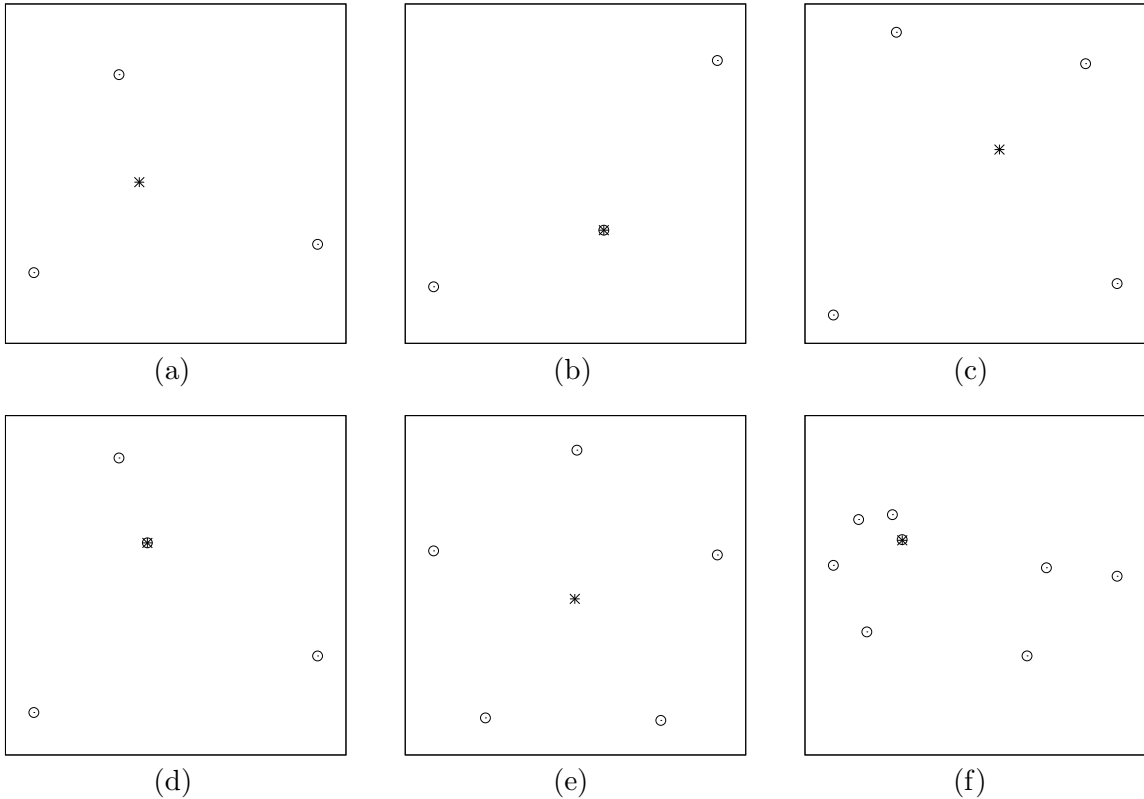
DEFINITION 26 (Continuous L^1 median). Let γ be a normalised regular density on \mathbb{R}^n . The L^1 median of γ is given by

$$\text{med}_{L^1}(\gamma) := \underset{\boldsymbol{\mu} \in \mathbb{R}^n}{\text{argmin}} E_{\gamma}^{L^1}(\boldsymbol{\mu}), \quad E_{\gamma}^{L^1}(\boldsymbol{\mu}) := \int_{\mathbb{R}^n} \gamma(\mathbf{x}) \|\boldsymbol{\mu} - \mathbf{x}\| \, d\mathbf{x}. \quad (36)$$

A generalisation to distribution-valued densities γ is again possible. We do not detail this here but remark that in the case if γ is concentrated on a straight line (i.e. essentially a single-layer distribution along this line), also the continuous L^1 median reproduces its univariate counterpart.

In [28] the L^1 median with Euclidean norm $\|\cdot\|$ as defined above is called *geometric median*, whereas the componentwise median (thus, the L^1 median with city-block metric) is called *arithmetic median*.

Equivariance. By its definition via distances, the L^1 median (with Euclidean distances as discussed above) is obviously equivariant w.r.t. Euclidean transformations of the data. This equivariance is extended to similarity transformations by noticing that scalings just entail scalings of the objective function $E_{\mathcal{X}}^{L^1}$ or $E_{\gamma}^{L^1}$, respectively. However, the L^1 median is not equivariant under any larger transformation group, which is a substantial difference to the univariate median with its very general monotonic equivariance.



Legend: \circ Data points $*$ L^1 median

Figure 1: Simple point sets with their L^1 medians. **(a)** In a triangle with no angle of 120 degrees or greater, the L^1 median is the Fermat-Torricelli point from which all sides of the triangle are seen under 120 degree angles. – **(b)** In a triangle with one angle greater or equal 120 degrees, the obtuse corner is the L^1 median. – **(c)** In a convex quadrilateral, the intersection point of the diagonals is the L^1 median. – **(d)** From four points with a triangle as convex hull, the inner data point is the L^1 median. – **(e)** Regular pentagon; the L^1 median is in the symmetry centre. – **(f)** A configuration of 8 points the L^1 median of which is one of the data points.

As a consequence, the use of the L^1 median always relies on a Euclidean structure in the data space. Wherever this structure is not naturally given, it is implicitly imposed on the data and not justified. For example, if the dimensions of the data space \mathbb{R}^n actually refer to incommensurable quantities (such as physical quantities measured by different units of measurement), L^1 median processing is not sound from a modelling perspective as its results depend on arbitrary choices of the relative scales between these dimensions. The componentwise median (L^1 median with city-block distances) would be a more plausible option in such a case, see also [28].

Algorithmic aspects. The basic idea of algorithms for the efficient calculation of L^1 medians is an iterative weighted means computation. In each step, an estimate for the median is improved by calculating weights for the data points as their reciprocal distances to the

estimate; the weighted mean of the data points with these weights becomes the next estimate. Special treatment is required if the estimate coincides with one of the data points.

The original version of this algorithm was found by Weiszfeld in 1937 [77]. Reformulations and variants of this procedure, with corrections to the treatment of the special cases, are found in [8, 36, 35, 49, 50, 64]. A complete correct algorithm was published by Vardi and Zhang in 2000 [71, 72].

The algorithmic complexity of this procedure is $\mathcal{O}(N)$ per iteration; thus the overall computational cost depends on the number of iterations. Further algorithmic improvements are therefore directed at increasing the convergence speed, see e.g. [11, 21].

4.2 Oja Median

The restrictive equivariance properties of the L^1 median motivated researchers since the 1970s to consider alternative ways to generalise the median concept to multivariate data. In \mathbb{R}^n -valued data, including such of incommensurable (physical) dimensions, affine structure is in most cases justifiable from a modelling point of view, such that equivariance under affine transformations is an appropriate choice to overcome the main weakness of the L^1 median.

Despite not being the first concept of this kind (in fact, the half-space and convex-hull-stripping medians discussed later in this section preceded it), the *simplex median* introduced by Oja [46, 47], nowadays mostly termed *Oja median*, is particularly close to the L^1 concept discussed before as it generalises the same minimisation property (4), (15) of the univariate median but in a different way.

Discrete data. The essential observation underlying Oja’s definition is that the distances $|\mu - x_i|$ in (4) can be interpreted as interval lengths, thus, one-dimensional simplex volumes. Transferring this interpretation to higher dimensions yields the following definition of a multivariate median.

DEFINITION 27 (Discrete Oja median). Let $\mathcal{X} = \{\mathbf{x}_1, \dots, \mathbf{x}_N\}$ be a finite multiset of data points $\mathbf{x}_i \in \mathbb{R}^n$ ($n \geq 2$). The *simplex median* or *Oja median* of \mathcal{X} is defined as

$$\begin{aligned} \text{med}_{\text{Oja}}(\mathcal{X}) &:= \underset{\boldsymbol{\mu} \in \mathbb{R}^n}{\text{argmin}} E_{\mathcal{X}}^{\text{Oja}}(\boldsymbol{\mu}), \\ E_{\mathcal{X}}^{\text{Oja}}(\boldsymbol{\mu}) &:= \sum_{1 \leq i_1 < \dots < i_n \leq N} |[\boldsymbol{\mu}, \mathbf{x}_{i_1}, \dots, \mathbf{x}_{i_n}]|, \end{aligned} \quad (37)$$

where $[\boldsymbol{\mu}, \mathbf{x}_{i_1}, \dots, \mathbf{x}_{i_n}]$ denotes the simplex spanned by the $n + 1$ points $\boldsymbol{\mu}, \mathbf{x}_{i_1}, \dots, \mathbf{x}_{i_n} \in \mathbb{R}^n$ and $|[\dots]|$ its volume.

To generalise (37) to weighted countable sets, simplices must be weighted with the product of the weights of all participating data points. The following considerations are written for the unweighted case but can be generalised to the weighted case.

In the bivariate case ($n = 2$), the median $\boldsymbol{\mu}$ thus minimises the area sum of all triangles $[\boldsymbol{\mu}, \mathbf{x}_i, \mathbf{x}_j]$; for $n = 3$ a sum of tetrahedron volumes is minimised etc.

Unlike the L^1 median, the Oja median is not defined anymore if the data in \mathcal{X} lie on a hyperplane, since in this case all simplices degenerate to zero volume for whatever $\boldsymbol{\mu}$ on the same hyperplane. Still, if in such a case the data set \mathcal{X} is enlarged by adding to each data point of \mathcal{X} a duplicate which is just shifted by $\varepsilon \mathbf{v}$, with the same $\varepsilon > 0$ for all data points and

\mathbf{v} being a vector transversal to the hyperplane containing \mathcal{X} (such as its normal vector), i.e.

$$\mathcal{X}_{\varepsilon\mathbf{v}} := \mathcal{X} \cup (\mathcal{X} + \varepsilon\mathbf{v}) , \quad (38)$$

then the Oja median of $\mathcal{X}_{\varepsilon\mathbf{v}}$ approaches for $\varepsilon \rightarrow 0$ the $(n - 1)$ -dimensional Oja median in the hyperplane of \mathcal{X} . In particular, the univariate median of data lying on a straight line is approximated from the 2-dimensional Oja median by this procedure.

For data that span \mathbb{R}^n , the Oja median will still sometimes be non-unique: For example, for three non-collinear points in the plane, the entire triangle with the data points as vertices consists of minimisers of $E_{\mathcal{X}}^{\text{Oja}}$.

As observed in [45], each of the simplex volume functions $v_{i_1, \dots, i_n} := |[\boldsymbol{\mu}, \mathbf{x}_{i_1}, \dots, \mathbf{x}_{i_n}]|$ is a convex function and consists of two linear regions separated by the hyperplane H_{i_1, \dots, i_n} spanned by $\mathbf{x}_{i_1}, \dots, \mathbf{x}_{i_n}$, where it has a kink. Therefore, $E_{\mathcal{X}}^{\text{Oja}}$ is also convex, and linear within each of the regions into which \mathbb{R}^n is split by the hyperplanes H_{i_1, \dots, i_n} for all (i_1, \dots, i_n) . As an interesting consequence there exists always at least one minimiser of $E_{\mathcal{X}}^{\text{Oja}}$ that is the intersection of n such hyperplanes. All minimisers with this property are vertices of a convex polygon, and the entire set of minimisers is their convex hull, i.e. the entire polygon. This is analogous to the fact that the univariate median set from (4) always contains at least one data point and is the convex hull of all data points with this property (at most two points in the univariate case).

In Figure 2, Oja medians of some simple point configurations are shown.

Continuous data. The definition of the Oja median transfers in an obvious way to the continuous setting.

DEFINITION 28 (Continuous Oja median). Let γ be a normalised regular density on \mathbb{R}^n . The *Oja median* of γ is defined by

$$\begin{aligned} \text{med}_{\text{Oja}}(\gamma) &:= \underset{\boldsymbol{\mu} \in \mathbb{R}^n}{\text{argmin}} E_{\gamma}^{\text{Oja}}(\boldsymbol{\mu}) , \\ E_{\gamma}^{\text{Oja}}(\boldsymbol{\mu}) &:= \int_{\mathbb{R}^n} \dots \int_{\mathbb{R}^n} |[\boldsymbol{\mu}, \mathbf{x}_1, \dots, \mathbf{x}_n]| \, d\mathbf{x}_1 \dots d\mathbf{x}_n . \end{aligned} \quad (39)$$

Equivariance. Affine equivariance of the Oja median is guaranteed by its construction.

Algorithmic aspects. The computational complexity of the Oja median computation increases with dimension: Already an evaluation of the objective function $E_{\mathcal{X}}^{\text{Oja}}(\boldsymbol{\mu})$ takes $\mathcal{O}(N^n)$ operations. Building on the geometric property mentioned above, [45, 53] develop algorithms that allow to compute the exact Oja median of N data points in n dimensions with $\mathcal{O}(nN^n \log N)$, or an approximation with stochastic accuracy guarantee in $\mathcal{O}(5^n/\varepsilon^2)$ where ε is a confidence radius in L^∞ sense. An $\mathcal{O}(N \log^3 N)$ algorithm for the bivariate Oja median is stated in [1, 2].

4.3 Transformation–Retransformation L^1 Median

As an alternative to the computational expensive Oja median, Chakraborty and Chaudhuri [16] proposed a standardisation procedure that allows to combine the computational efficiency of the L^1 median with affine equivariance. Their idea was to standardise a given data set

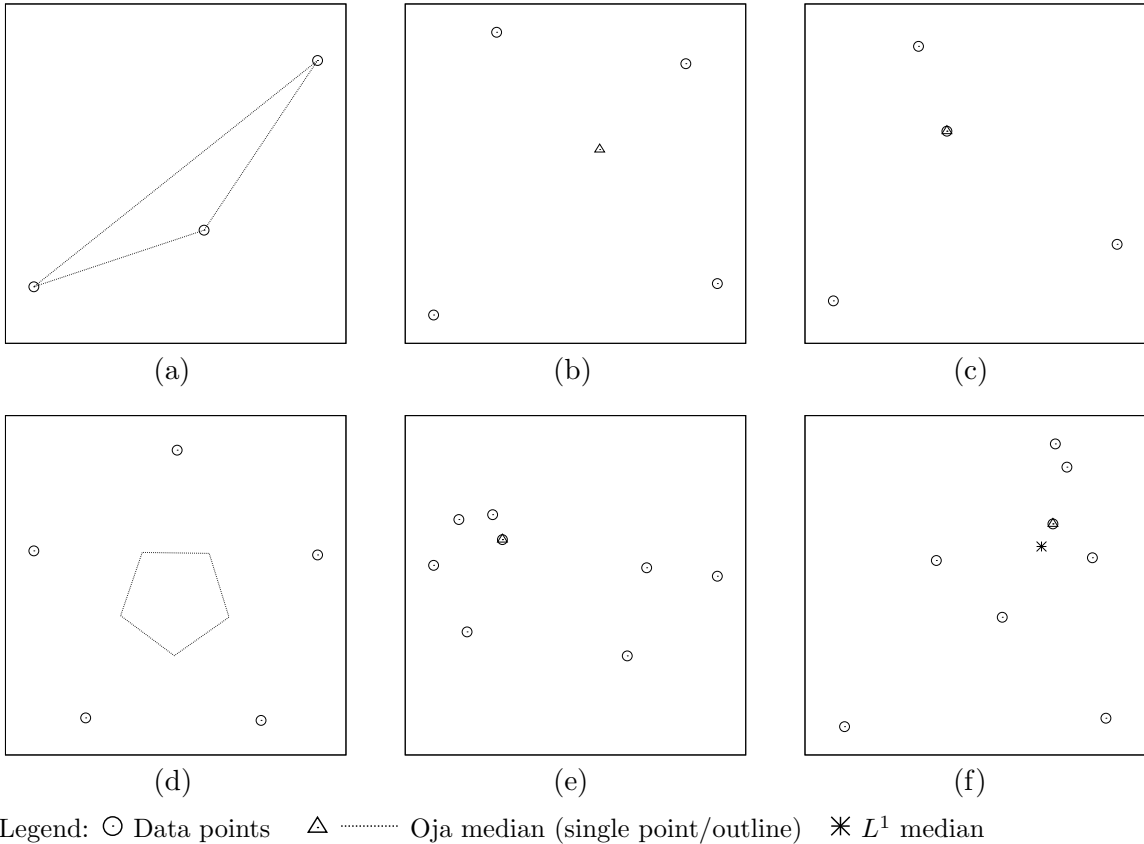


Figure 2: Simple point sets with their Oja medians. **(a)** For three data points, the Oja median set is the entire triangle spanned by these points. – **(b)** In a convex quadrilateral, the intersection point of the diagonals is the Oja median. – **(c)** From four points with a triangle as convex hull, the inner data point is the Oja median. – **(d)** Regular pentagon; the intersection points of the diagonals with the enclosed smaller pentagon form the Oja median set. – **(e)** Same configuration of 8 points as in Figure 1(f). The Oja median coincides with the L^1 median in one of the data points. – **(f)** Another configuration of 8 data points with Oja median. In this case, the Oja median is one of the data points where the L^1 median (also shown) is not.

by an affine transformation to a configuration that is uniquely determined up to Euclidean transformations.

The resulting affine equivariant median was further analysed in [30]. The standardisation procedure was discussed in a broader context of equivariance concepts in [63].

Discrete data. Applying the affine normalisation procedure to finite multisets in \mathbb{R}^n ($n \geq 2$) yields the following definition.

DEFINITION 29 (Discrete transformation–retransformation L^1 median). Let $\mathcal{X} = \{\mathbf{x}_1, \dots, \mathbf{x}_N\}$ be a finite multiset of data points $\mathbf{x}_i \in \mathbb{R}^n$ ($n \geq 2$). The *transformation–retransformation L^1 median* of \mathcal{X} is

$$\text{med}_{\text{TRL}^1}(\mathcal{X}) := T^{-1} \text{med}_{L^1}(T(\mathcal{X})), \quad (40)$$

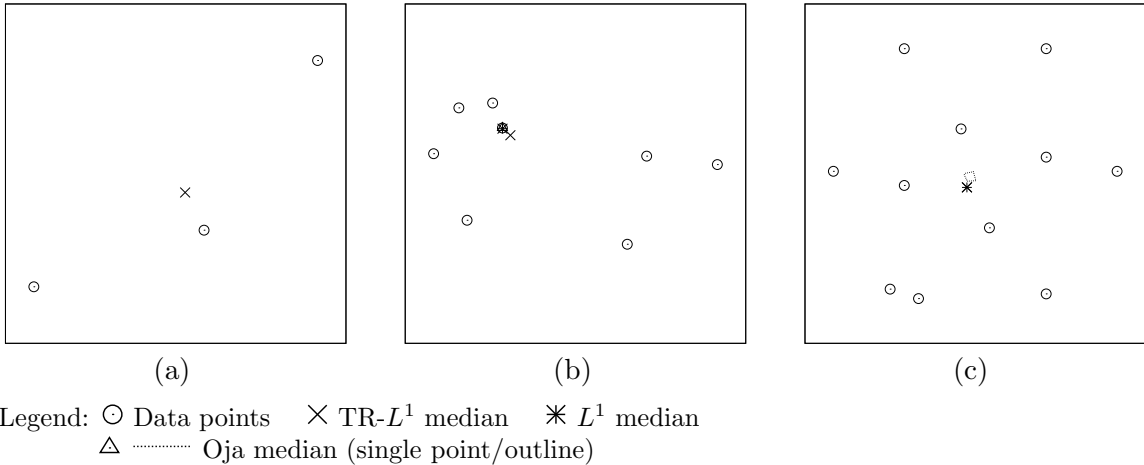


Figure 3: Simple point sets with their transformation–retransformation L^1 medians. (a) For three data points, the transformation–retransformation L^1 median is always in their barycentre. – (b) Same configuration of 8 points as in Figures 1(f) and 2(e). Unlike the L^1 and Oja median, the transformation–retransformation L^1 median is none of the data points. – (c) A sample configuration of 11 data points with transformation–retransformation L^1 , standard L^1 and Oja median. The first two medians are visually indistinguishable here.

where T denotes an affine transformation, and $T(\mathcal{X})$ its element-wise application to \mathcal{X} , that is chosen such that $T(\mathcal{X})$ has a unit covariance matrix \mathbf{I} .

If the symmetric positive semidefinite covariance matrix

$$C(\mathcal{X}) := \sum_{i=1}^N \sum_{j=1}^N (\mathbf{x}_i - \mathbf{x}_j)(\mathbf{x}_i - \mathbf{x}_j)^\top, \quad (41)$$

is regular (thus, positive definite), it is sufficient to choose $T := C(\mathcal{X})^{-1/2}$ because one has then

$$\begin{aligned} C(T(\mathcal{X})) &= \sum_i \sum_j (T\mathbf{x}_i - T\mathbf{x}_j)(T\mathbf{x}_i - T\mathbf{x}_j)^\top \\ &= T C(\mathcal{X}) T^\top = C(\mathcal{X})^{-1/2} C(\mathcal{X}) C(\mathcal{X})^{-1/2} = \mathbf{I}. \end{aligned} \quad (42)$$

It is obvious that the transformation–retransformation L^1 median is undefined if all \mathbf{x}_i lie on the same hyperplane, as the covariance matrix is singular in this case. (The same limiting procedure as for the Oja median may be used to recover from this problem.) In all other cases, the covariance matrix is positive definite, and the transformation–retransformation L^1 median is uniquely defined, based on the same property of the standard L^1 median.

In Figure 3, some examples of transformation–retransformation L^1 medians are shown.

Continuous data. Transfer of the procedure to the space-continuous case depends on the existence of the covariance matrix of the density, which is certainly fulfilled if γ is compactly supported.

DEFINITION 30 (Continuous transformation–retransformation L^1 median). Let γ be a normalised regular density for which the covariance matrix

$$C(\gamma) := \int_{\mathbb{R}^n} \int_{\mathbb{R}^n} \gamma(\mathbf{x}) \gamma(\mathbf{y}) (\mathbf{x} - \mathbf{y})(\mathbf{x} - \mathbf{y})^\top d\mathbf{x} d\mathbf{y} \quad (43)$$

exists and is positive definite, the *transformation–retransformation L^1 median* of γ is defined as

$$\text{med}_{\text{TRL}^1}(\gamma) := T^{-1} \text{med}_{L^1}(\gamma^T), \quad T := C(\gamma)^{-1/2} \quad (44)$$

with

$$\gamma^T(\mathbf{x}) := \det T \cdot \gamma(T\mathbf{x}). \quad (45)$$

As for the L^1 median, we do not detail the case of distribution-valued densities but notice that for γ concentrated on a straight line the covariance matrix will again become singular, preventing the definition of the transformation–retransformation L^1 median.

Equivariance. Affine equivariance of the transformation–retransformation L^1 median is guaranteed by its construction.

Algorithmic aspects. The transformation–retransformation median of a finite multiset can be computed using the efficient algorithms for L^1 medians, with the additional effort of computing the covariance matrix ($\mathcal{O}(N^2)$) and applying it to the data ($\mathcal{O}(N)$).

4.4 Half-Space Median

The *half-space median* was first conceived by Tukey [70]. It generalises the half-line characterisation of the univariate median as given by (3), (7), (11).

Discrete data. Following [66, 70], we introduce the half-space depth $d_{\mathcal{X}}^{\text{HS}}(\mathbf{y})$ of a point $\mathbf{y} \in \mathbb{R}^n$ w.r.t. a finite multiset \mathcal{X} of data points in \mathbb{R}^n as the minimal number of data points contained in a closed half-space containing \mathbf{y} . In fact, it is sufficient to minimise over half-spaces the boundary hyperplane of which goes through \mathbf{y} . Further following [66, 70], the half-space median then is the point of maximal half-space depth.

Characterising oriented hyperplanes by their unit normal vectors $\mathbf{z} \in S^{n-1} = \{\mathbf{x} \in \mathbb{R}^n \mid \|\mathbf{x}\| = 1\}$, we have the following definition.

DEFINITION 31 (Discrete half-space median). Let \mathcal{X} be a finite multiset in \mathbb{R}^n . For any $\mathbf{y} \in \mathbb{R}^n$, the *half-space depth* of \mathbf{y} w.r.t. \mathcal{X} is

$$d_{\mathcal{X}}^{\text{HS}}(\mathbf{y}) := \min_{\mathbf{z} \in S^{n-1}} \#\{\mathbf{x} \in \mathcal{X} \mid \mathbf{z}^T(\mathbf{x} - \mathbf{y}) \geq 0\}. \quad (46)$$

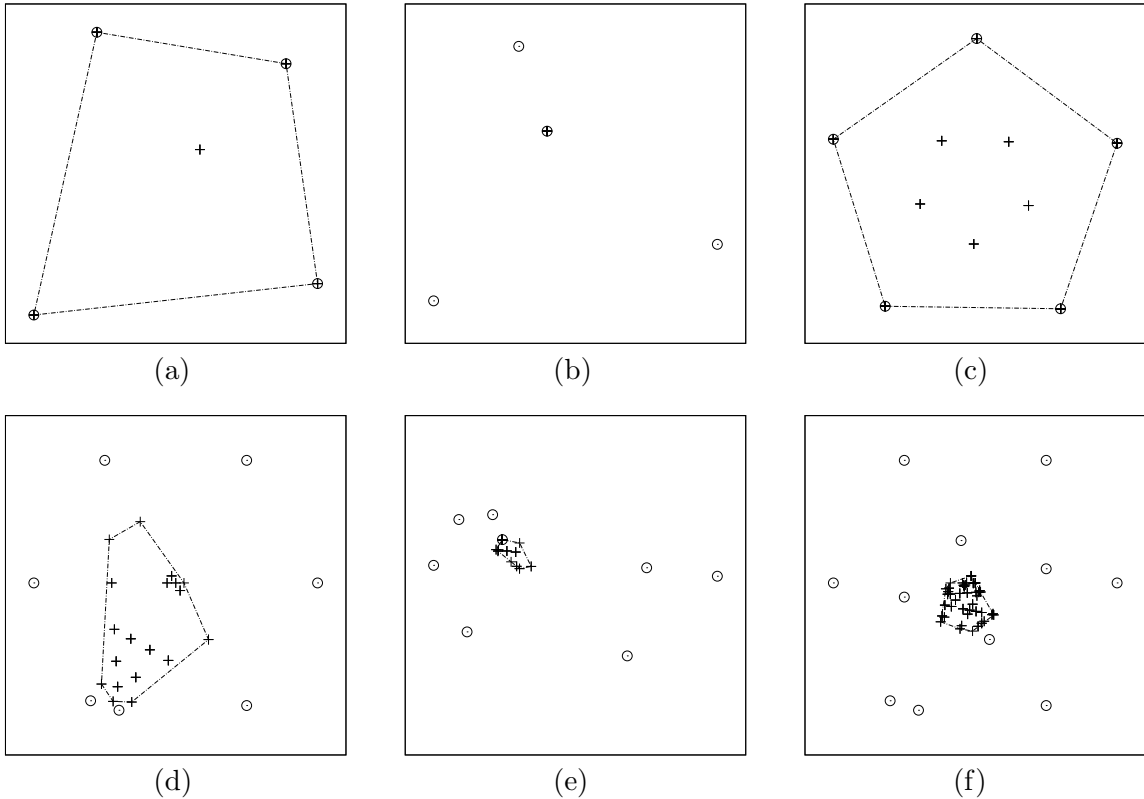
The *half-space median* of \mathcal{X} is given by

$$\text{med}_{\text{HS}}(\mathcal{X}) := \operatorname{argmax}_{\boldsymbol{\mu} \in \mathbb{R}^n} d_{\mathcal{X}}^{\text{HS}}(\boldsymbol{\mu}). \quad (47)$$

A generalisation of this definition to countable sets \mathcal{X} with weights w is straightforward by replacing the cardinality $\#$ with the sum of weights in the respective sets.

Similar as for the Oja median, the half-space median set always contains at least one intersection point of n hyperplanes H_{i_1, \dots, i_n} going through n data points, and the entire set of minimisers is the convex hull of all intersection points with this property. However, unlike for the Oja median, some intersection points may also lie in the interior of the set of minimisers.

If all data of \mathcal{X} lie on a hyperplane in \mathbb{R}^n , their half-space median automatically coincides with their half-space median in $n - 1$ dimensions.



Legend: \odot Data points $+$ ----- Half-space median (single point/outline)

Figure 4: Simple point sets with their half-space medians. If the half-space median set consists of more than one point, we show additionally all those intersection points of lines between data points that are contained in the half-space median set. **(a)** For four points spanning a convex quadrilateral, the entire quadrilateral is the half-space median set. – **(b)** From four points with a triangle as convex hull, the inner data point is the half-space median. – **(c)** Regular pentagon; the entire pentagon is the half-space median set. – **(d)** Sample configuration of 7 points with their half-space median. – **(e)** Same configuration of 8 points as in Figure 1(f). The half-space median set is a region including one of the data points (which is also the L^1 and Oja median) on its boundary. – **(f)** Configuration of 11 data points (same as in Figure 3(c)) with half-space median set.

In Figure 4, half-space medians of some simple point configurations are shown.

Continuous data. The half-space median of continuous data has been considered e.g. in [56].

DEFINITION 32 (Continuous half-space median). Let γ be a normalised regular density in \mathbb{R}^n . For any $\mathbf{y} \in \mathbb{R}^n$, the *half-space depth* of \mathbf{y} w.r.t. γ is

$$d_{\gamma}^{\text{HS}}(\mathbf{y}) := \min_{z \in \mathbb{S}^{n-1}} \int_{H_{\mathbf{y},z}^+} \gamma(\mathbf{x}) \, d\mathbf{x} \quad (48)$$

where $H_{\mathbf{y}, \mathbf{z}}^+ := \{\mathbf{x} \in \mathbb{R}^n \mid \mathbf{z}^\top(\mathbf{x} - \mathbf{y}) \geq 0\}$ denotes the half-space separated by a hyperplane with normal vector \mathbf{z} through \mathbf{y} . The *half-space median* of γ is then defined as

$$\text{med}_{\text{HS}}(\gamma) := \operatorname{argmax}_{\boldsymbol{\mu} \in \mathbb{R}^n} d_\gamma^{\text{HS}}(\boldsymbol{\mu}). \quad (49)$$

Equivariance. In discussions of the equivariance properties of the half-space median in the literature, emphasis is mostly laid on the affine equivariance of the half-space median. However, in [65] equivariance of the half-space median under a larger transformation class is proven, see also [66]. The transformations discussed there are characterised by the requirement that images of half-spaces containing $\boldsymbol{\mu}$, and pre-images of half-spaces not containing $\boldsymbol{\mu}$ must be convex.

Whereas this class of transformations is hard to describe in closed form, we point out a smaller class of transformations under which the half-space median is equivariant: Notice that the definition of half-space depth relies on nothing but the splitting of \mathbb{R}^n into half-spaces by hyperplanes, and the belonging of data points to these half-spaces. The preservation of hyperplanes is what characterises projective transformations. The caveat is that these transformations act on the larger (and non-orientable) projective space \mathbb{P}^n , which extends \mathbb{R}^n by a hyperplane at infinity. Nevertheless, projective transformations do not change the relation between points and the hyperplanes relevant for defining the half-space median as long as no point in the convex hull of the data points is taken to infinity.

Thus, the half-space median of a data multiset is equivariant under all projective transformations that do not take any point in its convex hull to the infinite hyperplane. Note that this restricted class of projective transformations is not a group; nevertheless, the closed-form representation of projective transformations can be used.

On \mathbb{R}^n , a general projective transformation T is given by a regular matrix $\hat{P} \in \text{GL}(n+1, \mathbb{R})$ which we write as

$$\hat{P} = \begin{pmatrix} P & \mathbf{q} \\ \mathbf{r}^\top & s \end{pmatrix} \quad (50)$$

with an $n \times n$ -matrix P , two vectors $\mathbf{q}, \mathbf{r} \in \mathbb{R}^n$ and a number $s \in \mathbb{R}$, and transforms points $\mathbf{x} \in \mathbb{R}^n$ with $\mathbf{r}^\top \mathbf{x} + s \neq 0$ via

$$T\mathbf{x} = \frac{P\mathbf{x} + \mathbf{q}}{\mathbf{r}^\top \mathbf{x} + s}. \quad (51)$$

Any matrix $\lambda \hat{P}$ with $\lambda \in \mathbb{R} \setminus \{0\}$ describes the same transformation T . (Alternatively, a unique \hat{P} can be associated to each T by choosing $\hat{P} \in \text{SL}(n+1, \mathbb{R})$.)

The half-space median of a finite multiset \mathcal{X} is then equivariant w.r.t. T if $\mathbf{r}^\top \mathbf{x} + s$ vanishes nowhere in the convex hull $[\mathcal{X}]$.

Algorithmic aspects. Like the computation of the Oja median, that of the half-space median is algorithmically not convenient. In the bivariate case the half-space depth $d_{\mathcal{X}}^{\text{HS}}(\mathbf{y})$ of a point can be computed by angular sorting of the data points w.r.t. \mathbf{y} in $\mathcal{O}(N \log N)$ time, followed by a linear-time computation to find the half-plane orientation with minimal number of points, see [54, 58]. Using a strategy for restricting the core part of the computation to a smaller set, [13] obtains an algorithm with complexity $\mathcal{O}(N + K \log K)$, where K is the actual depth.

To compute the half-space median by a direct approach requires up to $\mathcal{O}(N^4)$ evaluations of the depth (for all intersection points of lines connecting two data points), making the total complexity $\mathcal{O}(N^5 \log N)$ [54] with the $\mathcal{O}(N \log N)$ depth algorithm. By an improved selection procedure for intersection points, [55, 58] reduce the complexity to $\mathcal{O}(N^2 \log N)$.

Another approach to computing the half-space median uses algorithms that compute the convex sets of points with half-space depth $\geq K$ for given K . In [41], a divide-and-conquer algorithm is described that allows to achieve this goal in $\mathcal{O}(N \log^4 N)$. Combined with a bisection strategy to find the largest K for which the respective set is non-empty, this yields an $\mathcal{O}(N \log^5 N)$ algorithm for the bivariate half-space median [41]. In [37] an $\mathcal{O}(N \log^3 N)$ algorithm for the bivariate half-space median is stated.

An extension of the angular sorting idea to $n > 2$ via projections yields $\mathcal{O}(N^{n-1} \log N)$ complexity for the depth computation [54, 57]; however, also the number of depth evaluations increases since $\mathcal{O}(N^{\binom{n}{2}})$ intersections of n hyperplanes occur. In [57] approximative algorithms for the depth computation in higher dimensions with lower complexity are proposed. A stochastic algorithm by Chan [17] based on linear programming reaches an average (expected) $\mathcal{O}(N \log N + N^{n-1})$ computation time for the half-space median computation in dimension n .

4.5 Convex-Hull-Stripping Median

Generalising the extremum-stripping formulations for the multivariate median, Barnett's 1976 paper [10] together with its subsequent discussion by Seheult et al. [62] establish another geometric concept of a multivariate median. Extremal points of the convex hull of the data herein take the role of the extrema in the univariate process described in Definition 2.

Discrete data. For simplicity, we state the following definition for a set \mathcal{X} , i.e. without multiplicities.

DEFINITION 33 (Discrete convex-hull-stripping median). Let \mathcal{X} be a finite set of data points from \mathbb{R}^n . Define a series $(\mathcal{X}^k)_{k=0,1,2,\dots}$ of sets as follows: Start with the given data $\mathcal{X}^0 := \mathcal{X}$. Continue by deleting in each step $k \geq 1$ those data points from \mathcal{X}^{k-1} that are vertices of its convex hull boundary, i.e. with V^{k-1} denoting the set of boundary vertices, set $\mathcal{X}^k := \mathcal{X}^{k-1} \setminus V^{k-1}$. This is repeated until (after finitely many steps) an empty set is obtained. If $\mathcal{X}^k = \emptyset \neq \mathcal{X}^{k-1}$, the *convex-hull-stripping median* of \mathcal{X} is defined as the convex hull of \mathcal{X}^{k-1} ,

$$\text{med}_{\text{CHS}}(\mathcal{X}) := [\mathcal{X}^{k-1}]. \quad (52)$$

When generalising this definition to multisets \mathcal{X} , one has to decide whether multiple copies of a data point are deleted in one step, or one copy per step, when the convex hull boundary reaches this point. The latter might appear closer to what is done in the univariate extremum-stripping procedure but whatever choice is made makes the process discontinuous with regard to the input data, i.e. arbitrary small variations of the data can lead to the convex-hull-stripping median jumping to another value (set). Discontinuities also occur at configurations where one data point crosses a face of the convex hull in some step during the procedure. Thus, the convex-hull-stripping median does not depend continuously on the given data points.

Again, when all data points of \mathcal{X} are located on a hyperplane, their convex-hull-stripping median in n dimensions coincides with its counterpart in $n-1$ dimensions: Although in such a

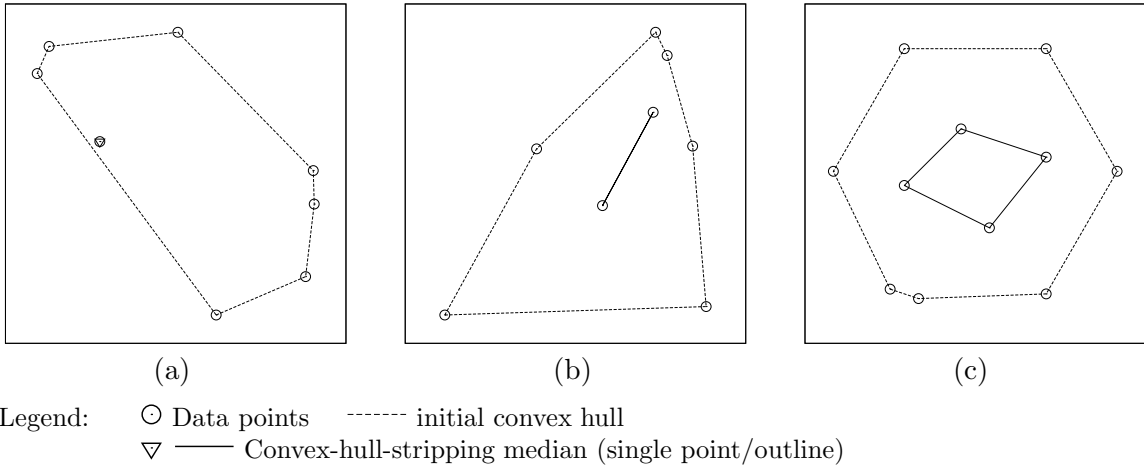


Figure 5: Simple point sets with their convex-hull-stripping medians. **(a)** A configuration of 8 data points with a unique convex-hull-stripping median. – **(b)** Same configuration of 8 points as in Figure 2(f); the convex-hull-stripping median set is a line segment. – **(c)** Same configuration of 11 data points as in Figure 4(f). Here, the median set is spanned by four points.

case in each step all data points are located on the boundary of the convex hull, the stripping process is designed to delete only vertices but not those data points lying somewhere on the facets of the (then degenerated) polytope.

In Figure 5, we show some point configurations with their convex-hull-stripping medians. An additional comparison of all five multivariate median concepts discussed is shown in Figure 6.

Continuous data. Unlike for the previously discussed multivariate medians, a space-continuous formulation for the convex-hull-stripping median is not at all obvious. As in the univariate case, where a system of ordinary differential equations (12) could be used to describe a continuous extrema-stripping process, one needs a process that moves the convex hull boundary in inward direction in a time-continuous manner, described by a partial differential equation.

In [82] a stochastic sampling procedure was proposed to derive a continuous process that can be considered the adequate continuous counterpart of the discrete convex-hull-stripping process. The results in [82] are restricted to the bivariate case, with the main finding being the following proposition. The curve evolution PDE in this result evolves a closed curve in inward direction, reducing it in finite time to a point which is called its vanishing point.

PROPOSITION 3 [82, Proposition 1]. *Let a piecewise smooth density $\gamma : \mathbb{R}^2 \rightarrow \mathbb{R}$ with compact support $\Omega_0 \subset \mathbb{R}^2$ in the Euclidean plane \mathbb{R}^2 be given. Assume that the boundary of Ω_0 is regular, and γ is differentiable on Ω_0 . Let the point set \mathcal{X} be a stochastic sampling of this density with sampling density $1/h^2$, i.e. there is on average one sampling point in an area in which the density integrates to h^2 . For $h \rightarrow 0$, the convex-hull-stripping median of the set \mathcal{X} asymptotically coincides with the vanishing point of the curve evolution*

$$\mathbf{c}_t(p, t) = \begin{cases} \gamma(\mathbf{c}(p, t))^{-2/3} \kappa(p, t)^{1/3} \mathbf{n}(p, t), & \mathbf{c}(p, t) \in \partial[\mathbf{c}(\cdot, t)], \\ 0 & \text{else} \end{cases} \quad (53)$$

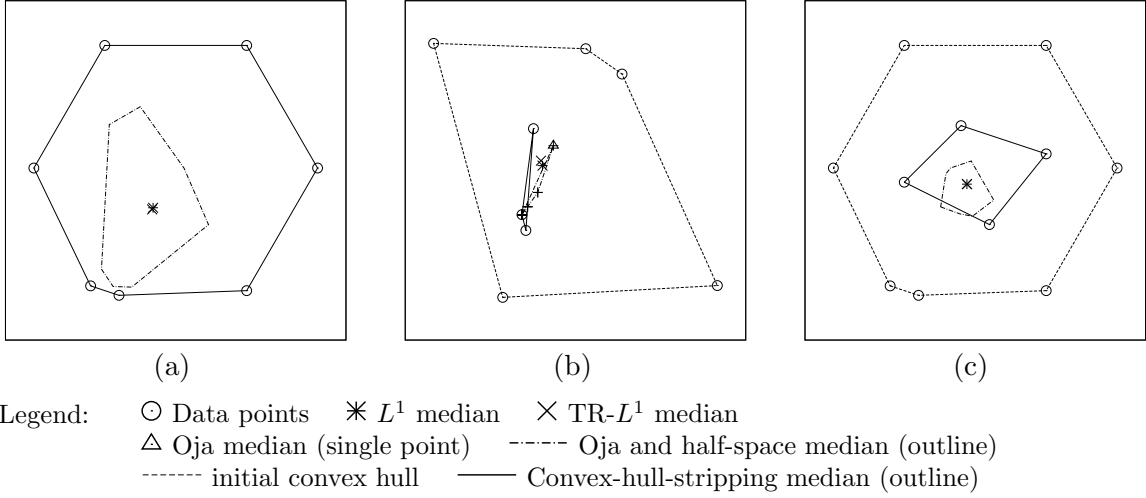


Figure 6: Comparison of multivariate median concepts. **(a)** Same data set of 7 points as in Figure 4(d) with multivariate medians. The Oja and half-space median sets coincide. The L^1 and transformation–retransformation L^1 medians differ but their distance is extremely small. – **(b)** A configuration of 8 points as in Figure 2(f); the convex-hull-stripping median set is a line segment. – **(c)** Same configuration of 11 data points as in Figure 4(f). Again, the Oja and half-space median sets coincide; L^1 and transformation–retransformation L^1 medians differ below visibility distance.

where $\mathbf{c} : [0, L] \times [0, T] \rightarrow \mathbb{R}^2$ is a curve evolution of closed curves with curve parameter $p \in [0, L]$ and evolution time $t \in [0, T]$, which is initialised at time $t = 0$ with the boundary of the support set, $\mathbf{c}_0 := \partial\Omega_0$. Furthermore, $\kappa(p, t)$ denotes the curvature and $\mathbf{n}(p, t)$ the inward normal vector of \mathbf{c} at (p, t) . At any time t , the evolution acts only on the part of \mathbf{c} that is on the boundary $\partial[\mathbf{c}]$ of the convex hull of \mathbf{c} .

By virtue of this proposition, one can define the convex-hull-stripping median of a density of compact support as follows.

DEFINITION 34 (Continuous convex-hull-stripping median). Let γ be a normalised regular density with compact support. Define the curve evolution \mathbf{c} as in Proposition 3. The vanishing point of this curve evolution is the *convex-hull-stripping median* of γ .

It is interesting to notice that (53) is a modification of the *affine curvature flow* PDE [3, 61]

$$\mathbf{c}_t(p, t) = \kappa(p, t)^{1/3} \mathbf{n}(p, t). \quad (54)$$

Note that affine curvature flow is an affine equivariant curve shrinking evolution. Its appearance in this context appears natural given the affine equivariant nature of the discrete convex-hull-stripping process.

The modification of (53) compared to (54) is twofold: On one hand, the evolution speed in the plane is weighted to account for the varying density γ ; on the other hand, its effect is

restricted to those parts of the boundary curve of the evolving support set that belong to the boundary of its convex hull.

The latter restriction is based on a non-local condition which adds complication to possible numeric approximations of the process. In [82] therefore a regularisation is proposed that allows to work without such a restriction and only on convex boundary curves:

PROPOSITION 4 [82, Corollary 1]. *Let the density γ with support Ω_0 , and the sampled point set \mathcal{X} with sampling density $1/h^2$ be given as in Proposition 3. Let $\tilde{\Omega}_0 \supseteq \Omega_0$ be a convex compact set with regular boundary. For $\varepsilon > 0$, define a piecewise smooth density γ_ε on $\tilde{\Omega}_0$ by $\gamma_\varepsilon(\mathbf{x}) = \gamma(\mathbf{x})$ for $\mathbf{x} \in \Omega_0$, $\gamma_\varepsilon(\mathbf{x}) = \varepsilon$ for $\mathbf{x} \in \tilde{\Omega}_0 \setminus \Omega_0$.*

For $h \rightarrow 0$, the convex-hull-stripping median of the set \mathcal{X} asymptotically coincides with the limit for $\varepsilon \rightarrow 0$ of the vanishing point of the curve evolution

$$\tilde{\mathbf{c}}_t(p, t) = \gamma_\varepsilon(\tilde{\mathbf{c}}(p, t))^{-2/3} \kappa(p, t)^{1/3} \mathbf{n}_{\tilde{\mathbf{c}}}(p, t) \quad (55)$$

where $\tilde{\mathbf{c}}$ is initialised at $t = 0$ with the convex closed curve $\partial\tilde{\Omega}_0$.

Algorithmic aspects. The core component of the convex-hull-stripping procedure for finite multisets is the computation of the convex hull. This problem is related to the half-space median computation as the convex hull consists of the points of non-zero half-space depth. Some sources mentioned above in the paragraph on half-space median algorithms therefore provide also algorithms that can be used here.

In the bivariate case, [41] shows that the convex hull of a finite multiset can be computed in $\mathcal{O}(N \log^4 N)$. Repeating this procedure at most $\mathcal{O}(N)$ times during the stripping procedure, the bivariate convex-hull-stripping median can be computed in $\mathcal{O}(N^2 \log^4 N)$.

For higher dimensions, the computation of halfspace depth in $\mathcal{O}(N^{n-1} \log N)$ can be used to compute the depth of all data points (and thereby the convex hull) in $\mathcal{O}(N^n \log N)$. The convex-hull-stripping median can then be computed with $\mathcal{O}(N^{n+1} \log N)$ effort.

Equivariance. In [66] only affine equivariance is mentioned for the convex-hull-stripping median. However, our argument for the half-space median above stays valid for the convex-hull-stripping median: The convex-hull-stripping procedure, too, relies solely on the splitting of \mathbb{R}^n into half-spaces by hyperplanes, and the incidence of data points with these half-spaces.

As a consequence, the convex-hull-stripping median is equivariant under the same sub-class of projective transformations as the half-space median.

In Figure 7 we demonstrate the restricted projective equivariance of half-space and convex-hull-stripping median and show that the other medians do not share this property. In this example, multivariate medians are computed from an original data set, Figure 7(a, b) and a projectively transformed version, Figure 7(c, d). After transforming the medians back, Figure 7(e, f), the half-space and convex-hull-stripping medians coincide with those from (a, b) whereas this is not true for the other three multivariate medians.

4.6 Remarks on Further Concepts

The list of multivariate median concepts discussed so far is not exhaustive. In [66] some more concepts are mentioned. Several of these approaches can be formulated similarly to the half-space median as maximisation of some depth of a median candidate point $\boldsymbol{\mu}$ w.r.t.

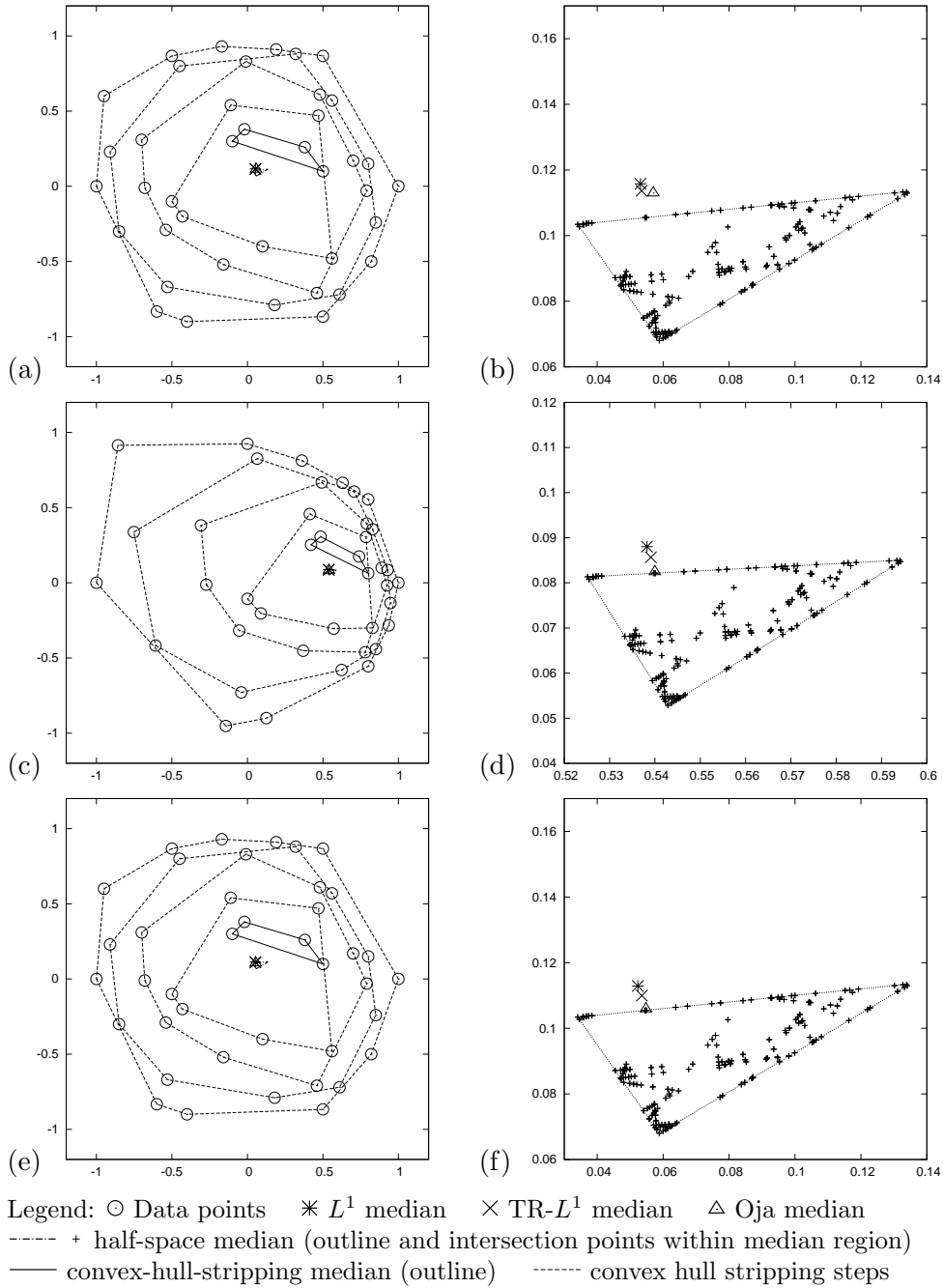


Figure 7: Comparison of multivariate median concepts. (a) Data set of 40 points with multivariate medians. – (b) Zoomed region from (a) showing the L^1 , transformation–retransformation L^1 , Oja and half-space median. Crosses in the half-space median area indicate further intersection points contained. – (c) Projective transformed data set from (a) and medians of transformed data. – (d) Zoomed region of (c). – (e) Data and medians from (c) transformed back. – (f) Zoomed region of (e).

the given data \mathcal{X} . Instead of the half-space depth, one can use e.g. the *simplicial depth*, i.e. the number of simplices with vertices from \mathcal{X} that contain $\boldsymbol{\mu}$, which is conceptually linked to the Oja median construction. Also variants of the Oja median objective function can be considered in which the simplex volumes are replaced by e.g. the height of $\boldsymbol{\mu}$ over the base of each simplex. As a modification of the convex-hull-stripping procedure, one can consider a minimal ellipsoid enclosing \mathcal{X} instead of the convex hull, and establish a stripping procedure that deletes just the data points on the boundary of this ellipsoid. Another variant is the *zonoid median* discussed in [22]. For more details and further variants see also the references in [22, 66].

5 Image Filtering of Multivariate Images

The first approaches to construct median filters for multivariate images go back to around 1990. In [5], by the name *vector median filter* a minimisation of the objective function of the L^1 median but restricted to the sample values is introduced, see also [73] for an application to video sequences. In modern nomenclature, compare [68], such a concept could rather be called a medoid. The actual L^1 median filter was brought to image processing in [67] for RGB colour images, and in [84] for matrix-valued images. The latter work was extended by some variants with other matrix norms instead of the Euclidean (thus, Frobenius) norm for matrices in [85] and transferred to colour images in [34] by mapping the RGB colour space to symmetric matrices. Affine equivariant medians as the basis for image filters were considered in [78].

5.1 L^1 Median

The application of the L^1 median to multivariate image data is fairly straightforward. In particular, the L^1 median of data in \mathbb{R}^n naturally decays into a lower-dimensional L^1 or univariate median if the data lie on a hyperplane or submanifold, it works for any dimensions of the image domain and data range.

5.2 Affine Equivariant Medians

The affine equivariant medians considered in Section 4 are in the one or other way sensitive to the dimension of the space actually spanned by the data values. When applying these medians to the filtering of multivariate images, the dimension m of the image domain and the dimension n of the data space therefore need closer consideration.

Dimensionality considerations. For bivariate planar images ($m = n = 2$) as well as for trivariate volume images ($m = n = 3$), and generally for every setting with $m \geq n$, the data values within the neighbourhood of any grid location will in generally span the data space, such that the affine equivariant medians can be applied straightforwardly.

This changes for $m < n$, which includes especially the practically relevant case of trivariate planar images, such as RGB colour images, which we will therefore discuss in the following for the Oja median. For general m, n with $m < n$ these considerations apply analogously.

A trivariate planar image in fact results from the discretisation of a function $\boldsymbol{u} : \mathbb{R}^2 \supset \Omega \rightarrow \mathbb{R}^3$, i.e. a parametrised surface in \mathbb{R}^3 . The values of \boldsymbol{u} in the neighbourhood of a given

location are therefore sampled from a small surface patch in \mathbb{R}^3 . For a noise-free image, the function \mathbf{u} can be assumed to be smooth, resulting in almost planar surface patches.

This implies that e.g. the 3D Oja median applied to the data points selected by a sliding window will be the minimiser of a sum of simplex volumes where virtually all of the simplices are almost degenerated, rendering the direct computation of the 3D Oja median unstable. On the other hand, the 2D Oja median, which minimises a sum of triangle areas, can easily be applied to these data. From the remarks in Section 4.2 it is evident that the 2D Oja median is also the proper limit case of the 3D Oja median when data collapse to a plane. Oja median filtering of trivariate images over planar domains should therefore be carried out by using the two-dimensional Oja objective function. This is proposed in [78, Section 3.3].

Spelling out the two-dimensional Oja median for three-dimensional (but almost planar) data yields

$$\text{med}_{\text{Oja}(2,3)}(\mathcal{X}) := \underset{\boldsymbol{\mu} \in \mathbb{R}^3}{\text{argmin}} \sum_{1 \leq i < j \leq N} |[\boldsymbol{\mu}, \mathbf{x}_i, \mathbf{x}_j]|. \quad (56)$$

Of course, the 2D Oja median $\text{med}_{\text{Oja}(2,3)}$ for general 3D data is not equivariant under affine transformations of \mathbb{R}^3 . However, the 2D Oja median of co-planar data from \mathbb{R}^3 is affine equivariant even with respect to affine transformations of \mathbb{R}^3 . Since the RGB triples being filtered are almost co-planar, it can be expected that a 2D Oja median filter for planar RGB images will display a good approximation to affine equivariance.

Alternatively, one could enlarge the data (multi-) set by adding shifted copies of all data points analogous to (38) to ensure full dimensionality of the data samples, compare [78, Section 2.1], and apply the three-dimensional Oja median.

For the transformation–retransformation L^1 median, the affine normalisation via the covariance matrix should be restricted to the plane of main variation of the data values.

6 PDE Limits of Multivariate Median Filters

In this section, we collect known results on PDE limits of space-continuous multivariate median filters that extend the result by Guichard and Morel [27] mentioned in Section 3.3.

6.1 General Definitions

To represent the results from [78, 79] in a more compact form, we start by generalising our definitions from Section 3.2 to multivariate images over domains of different dimensions.

DEFINITION 35 (Smooth multivariate image). Let $\Omega \subset \mathbb{R}^m$ be compact and equal to the closure of its interior. Let $\mathbf{u} : \Omega \rightarrow \mathbb{R}^n$ be a bounded smooth function on Ω . We call \mathbf{u} *n-variate m-dimensional smooth image with domain Ω* , or shortly *(m, n)-image*.

We denote by $D\mathbf{u}$ the Jacobian of \mathbf{u} , i.e. the $n \times m$ -tensor of its first-order derivatives, and by $D^2\mathbf{u}$ its Hessian, i.e. the $n \times n \times m$ -tensor of its second-order derivatives. We call $\mathbf{x} \in \Omega$ *regular point of \mathbf{u}* if $D\mathbf{u}(\mathbf{x})$ has maximal rank.

DEFINITION 36 (Multivariate image evolution). Let $\Omega \subset \mathbb{R}^m$ be as in Definition 35, and $[0, T] \subset \mathbb{R}$ an interval. The coordinates of Ω will be called *spatial coordinates*, the additional coordinate from $[0, T]$ *time coordinate*. Let $\mathbf{u} : \Omega \times [0, T] \rightarrow \mathbb{R}^n$ be a bounded smooth function. We call \mathbf{u} an *(m, n)-image evolution with spatial domain Ω* .

We denote by $D\mathbf{u}$ the spatial Jacobian of \mathbf{u} , i.e. the $n \times m$ -tensor of its first-order derivatives w.r.t. the spatial coordinates, and by $D^2\mathbf{u}$ its spatial Hessian, i.e. the $n \times n \times m$ -tensor of its second-order derivatives w.r.t the spatial coordinates.

By $\mathbf{u}(t^*)$ for $t^* \in [0, T]$ we denote the (m, n) -image with $\mathbf{u}(t^*)(\mathbf{x}) := \mathbf{u}(\mathbf{x}, t^*)$ for all $\mathbf{x} \in \Omega$.

The definitions for selectors and scaled selectors from Section 3.2 carry over verbatim if just the scalar-valued u in these definitions is replaced with the multivariate \mathbf{u} and the image domain $\Omega \subset \mathbb{R}^2$ with $\Omega \subset \mathbb{R}^m$.

The planar selector family \mathcal{D} from Section 3.2 can easily be generalised to arbitrary dimensions as the family $\mathcal{B}^m = \{B_\varrho^m \mid \varrho > 0\}$ of balls with radius ϱ given by $B_\varrho^m(\mathbf{x}) = \{\mathbf{y} \in \mathbb{R}^m \mid \|\mathbf{y} - \mathbf{x}\| \leq \varrho\}$. Also the amoeba families \mathcal{A}_β could be generalised in a similar way but this generalisation is not needed here.

Similarly, the definition of an aggregator can be generalised to integrable densities over \mathbb{R}^n . In particular, each of the space-continuous median operators introduced in Section 4 is an aggregator.

We give here just the adapted version of Definition 21.

DEFINITION 37 (Local filters). Let \mathbf{u} be an (m, n) -image with domain Ω , and S a selector for \mathbf{u} . Let $\mathbf{u}|S$ be the restriction of \mathbf{u} to $\Omega \cap S$, i.e. $\mathbf{u}|S : \Omega \cap S \rightarrow \mathbb{R}^n$, $(\mathbf{u}|S)(\mathbf{x}) = \mathbf{u}(\mathbf{x})$ for $\mathbf{x} \in \Omega \cap S$,

Let A be a Γ -aggregator on \mathbb{R}^n . If for each $\mathbf{x} \in \Omega$, the density $\gamma(\mathbf{u}|(S(\mathbf{x}))) : \mathbb{R}^n \rightarrow \mathbb{R}_0^+$ of the values of $\mathbf{u}|(S(\mathbf{x}))$ belongs to Γ , we define $A(\mathbf{u}, S) : \Omega \rightarrow \mathbb{R}^n$ by $A(\mathbf{u}, S)(\mathbf{x}) := A(\gamma(\mathbf{u}|(\mathbf{x} + S)))$ for all $\mathbf{x} \in \Omega$ and call it (A, S) -filtering of \mathbf{u} .

If Σ is a scaled selector for \mathbf{u} , and the $(A, \Sigma_{\mathbf{u}, \varrho})$ -filtering of \mathbf{u} exists for all $\varrho > 0$, we call the family of $(A, \Sigma_{\mathbf{u}, \varrho})$ -filterings the (A, Σ) -filtering of \mathbf{u} .

Adapted to the case of (m, n) -images, the definition of a regular PDE limit takes the following form.

DEFINITION 38 (Regular PDE limit). Let Σ be a scaled selector in \mathbb{R}^m , and A a Γ -aggregator on \mathbb{R}^n .

The second-order PDE $\mathbf{u}_t = F(D\mathbf{u}, D^2\mathbf{u})$ is the *regular PDE limit of (A, Σ) -filtering* with *time scale* $\tau(\varrho)$ if for each (m, n) -image \mathbf{u} the (A, Σ) -filtering exists, and if there exists an $\varepsilon > 0$ such that for each regular point \mathbf{x} of \mathbf{u} one has for $\varrho \rightarrow 0$

$$\frac{A(\mathbf{u}, \Sigma_{\mathbf{u}, \varrho})(\mathbf{x}) - \mathbf{u}(\mathbf{x})}{\tau(\varrho)} - F(D\mathbf{u}(\mathbf{x}), D^2\mathbf{u}(\mathbf{x})) = \mathcal{O}(\varrho^\varepsilon). \quad (57)$$

Since we will need a local version of this limit process in the following, we add the following definition that was omitted in the univariate case in Section 3.3.

DEFINITION 39 (Local PDE limit). Let Σ and A be as in Definition 38. Let \mathbf{u} be an (m, n) -image with a regular point \mathbf{x}_0 .

The second-order PDE $\mathbf{u}_t = F(D\mathbf{u}, D^2\mathbf{u})$ is the *local PDE limit of (A, Σ) -filtering* with *time scale* $\tau(\varrho)$ for \mathbf{u} at \mathbf{x}_0 if the (A, Σ) -filtering of \mathbf{u} at \mathbf{x}_0 exists, and if there exists an $\varepsilon > 0$ such that one has for $\varrho \rightarrow 0$

$$\frac{A(\mathbf{u}, \Sigma_{\mathbf{u}, \varrho})(\mathbf{x}_0) - \mathbf{u}(\mathbf{x}_0)}{\tau(\varrho)} - F(D\mathbf{u}(\mathbf{x}_0), D^2\mathbf{u}(\mathbf{x}_0)) = \mathcal{O}(\varrho^\varepsilon). \quad (58)$$

6.2 Bivariate Planar Images

We start now by considering bivariate planar images ($\mathbb{R}^2 \rightarrow \mathbb{R}^2$). As colour images usually have at least three channels, the practical relevance of bivariate images is limited, with planar optical flow fields as the most prominent exception. However, they are the most accessible case for theoretical analysis, and therefore the broadest range of asymptotic results are available for this setting.

Normalisations. All results on PDE limits of multivariate median filters reported in the following are obtained in two steps: First, an asymptotic analysis is carried out for a specific geometric situation where the Jacobian made up by the first derivatives of the multivariate image is aligned with coordinate directions. Second, this result is generalised to general geometric situations by using a transformation group depending on the equivariance properties of the respective median filter, i.e. a similarity or affine transformation.

For filtering processes that are just Euclidean/similarity equivariant, similarity transforms will be used. As a result, the PDE in the general case will naturally be stated in terms of *geometric coordinates* aligned with the principal directions of the structure tensor of the image. This applies obviously to standard L^1 median filtering. However, it happens also to be the case for amoeba median filtering even with affine equivariant multivariate medians because the amoeba structuring elements depend on the Euclidean structure of the image domain. In contrast, filtering processes with affine equivariance are normalised in the analysis by affine transformations. The general PDE in these cases is stated in standard coordinates because the geometric coordinates have no specific meaning in this context.

We give here the basic definitions for geometric coordinates and Euclidean normalisation.

DEFINITION 40 (Geometric coordinates). Let \mathbf{u} be a $(2, 2)$ -image and \mathbf{x} a regular location of \mathbf{u} . Let

$$\mathbf{J} := \mathbf{J}(\mathbf{D}\mathbf{u}(\mathbf{x})) := \nabla \mathbf{u} \nabla \mathbf{u}^T + \nabla \mathbf{v} \nabla \mathbf{v}^T = \mathbf{D}\mathbf{u}^T \mathbf{D}\mathbf{u} \quad (59)$$

where all derivatives are evaluated at \mathbf{x} . Then \mathbf{J} is called *structure tensor* of \mathbf{u} at \mathbf{x} . At each regular location \mathbf{x} , let $\boldsymbol{\eta}$, $\boldsymbol{\xi}$ be unit eigenvectors for the major and minor eigenvalues, respectively, of $\mathbf{J}(\mathbf{D}\mathbf{u}(\mathbf{x}))$. We call $\boldsymbol{\eta}$, $\boldsymbol{\xi}$ *geometric coordinates*.

The geometric coordinates are the spatial directions in the image domain Ω in which the function values of \mathbf{u} show the fastest and slowest change (measured by the Euclidean norm), and thus the closest analoga to the gradient and level line directions of univariate images, see [18]. In the univariate case, these coordinates occur naturally when describing curvature-based image evolutions such as (mean) curvature motion. The bivariate generalisations will be useful in representing some PDE evolutions arising from bivariate median filters.

DEFINITION 41 (Euclidean normalisation matrix). Let \mathbf{u} and \mathbf{x} be as in Definition 40. Define the matrix \mathbf{R} at location \mathbf{x} using the eigenvector matrix $\mathbf{P} := (\boldsymbol{\eta} \mid \boldsymbol{\xi})$ of the structure tensor, the Jacobian $\mathbf{D}\mathbf{u}$, and the directional derivatives of \mathbf{u} in the directions of the geometric coordinates as

$$\mathbf{R} := (\mathbf{D}\mathbf{u}^{-1})^T \mathbf{P} \text{diag}(\|\partial_{\boldsymbol{\eta}} \mathbf{u}\|, \|\partial_{\boldsymbol{\xi}} \mathbf{u}\|) . \quad (60)$$

We call \mathbf{R} *Euclidean normalisation matrix* of \mathbf{u} at \mathbf{x} .

The Euclidean normalisation matrix is a rotation matrix that allows to transform a bivariate planar image locally in such a way that its geometric coordinates are aligned to coordinate axes in the image domain Ω , and the directional derivatives along the geometric coordinates are aligned to coordinate axes in the range of image values.

L^1 **median.** As equivariance of L^1 median filtering is restricted to similarity transformations, its general PDE limit will be derived from a special geometric situation that can be reached by Euclidean transformations and is covered by the following lemma.

LEMMA 5 . [78, Lemma 1] For a (2,2)-image \mathbf{u} with a regular point \mathbf{x}_0 where $\mathbf{D}\mathbf{u}(\mathbf{x}_0) = \text{diag}(u_x, v_y)$ with $u_x \geq v_y > 0$ (i.e. $u_y = v_x = 0$), the local PDE limit of $(\text{med}_{L^1}, \mathcal{B}^2)$ -filtering of \mathbf{u} at \mathbf{x}_0 with time scale $\varrho^2/6$ is

$$u_t = Q_1\left(\frac{u_x}{v_y}\right)u_{xx} + Q_2\left(\frac{v_y}{u_x}\right)u_{yy} - \frac{2u_x}{v_y}Q_1\left(\frac{u_x}{v_y}\right)v_{xy}, \quad (61)$$

$$v_t = Q_2\left(\frac{u_x}{v_y}\right)v_{xx} + Q_1\left(\frac{v_y}{u_x}\right)v_{yy} - \frac{2v_y}{u_x}Q_1\left(\frac{v_y}{u_x}\right)u_{xy}. \quad (62)$$

The functions $Q_1, Q_2 : [0, \infty] \rightarrow \mathbb{R}$ are given by the quotients of elliptic integrals

$$Q_1(\lambda) = \frac{3 \iint_{D_1(\mathbf{0})} s^2 t^2 / (s^2 + \lambda^2 t^2)^{3/2} ds dt}{\iint_{D_1(\mathbf{0})} s^2 / (s^2 + \lambda^2 t^2)^{3/2} ds dt}, \quad (63)$$

$$Q_2(\lambda) = \frac{3 \iint_{D_1(\mathbf{0})} t^4 / (s^2 + \lambda^2 t^2)^{3/2} ds dt}{\iint_{D_1(\mathbf{0})} t^2 / (s^2 + \lambda^2 t^2)^{3/2} ds dt} \quad (64)$$

for $\lambda \in (0, \infty)$, together with the limits $Q_1(0) = Q_2(0) = 1$.

The elliptic integrals in the coefficient expressions $Q_1(\lambda)$ and $Q_2(\lambda)$ can in general not be evaluated in closed form. However, they are connected by

$$Q_2(\lambda) = 1 - Q_1(\lambda^{-1}). \quad (65)$$

Note that for $\lambda \rightarrow \infty$, $\lambda Q_1(\lambda)$ goes to zero such that the coefficients for v_{xy} in (61) and for u_{xy} in (62) are globally bounded for arbitrary u_x, v_y , and in the limit case $v_y = 0$ one has the decoupled PDEs $u_t = u_{yy}, v_t = v_{xx}$.

A general geometric situation can be normalised to the one described in the lemma by a Euclidean transformation in the image domain and data space which is given by the Euclidean normalisation matrix. The general PDE in the following proposition is obtained by reverting this transformation.

PROPOSITION 6 [78, Prop. 1]. For (2,2)-images \mathbf{u} , $(\text{med}_{L^1}, \mathcal{D})$ -filtering with the L^1 median as aggregator and the disc family \mathcal{D} as scaled selector has the regular PDE limit with time scale $\tau(\varrho) = \varrho^2/6$ given by

$$\mathbf{u}_t = \mathbf{S}(\mathbf{D}\mathbf{u})\mathbf{u}_{\eta\eta} + \mathbf{T}(\mathbf{D}\mathbf{u})\mathbf{u}_{\xi\xi} - 2\mathbf{W}(\mathbf{D}\mathbf{u})\mathbf{u}_{\xi\eta} \quad (66)$$

where $\boldsymbol{\eta}, \boldsymbol{\xi}$ are the geometric coordinates, and the coefficient matrices $\mathbf{S}(\mathbf{D}\mathbf{u})$, $\mathbf{T}(\mathbf{D}\mathbf{u})$ and $\mathbf{W}(\mathbf{D}\mathbf{u})$ are given by

$$\mathbf{S}(\mathbf{D}\mathbf{u}) := \mathbf{R} \text{diag} \left(Q_1 \left(\frac{\|\partial_{\boldsymbol{\eta}} \mathbf{u}\|}{\|\partial_{\boldsymbol{\xi}} \mathbf{u}\|} \right), Q_2 \left(\frac{\|\partial_{\boldsymbol{\eta}} \mathbf{u}\|}{\|\partial_{\boldsymbol{\xi}} \mathbf{u}\|} \right) \right) \mathbf{R}^T, \quad (67)$$

$$\mathbf{T}(\mathbf{D}\mathbf{u}) := \mathbf{R} \operatorname{diag} \left(Q_2 \left(\frac{\|\partial_\xi \mathbf{u}\|}{\|\partial_\eta \mathbf{u}\|} \right), Q_1 \left(\frac{\|\partial_\xi \mathbf{u}\|}{\|\partial_\eta \mathbf{u}\|} \right) \right) \mathbf{R}^\top, \quad (68)$$

$$\mathbf{W}(\mathbf{D}\mathbf{u}) := \mathbf{R} \begin{pmatrix} 0 & \frac{\|\partial_\eta \mathbf{u}\|}{\|\partial_\xi \mathbf{u}\|} Q_1 \left(\frac{\|\partial_\eta \mathbf{u}\|}{\|\partial_\xi \mathbf{u}\|} \right) \\ \frac{\|\partial_\xi \mathbf{u}\|}{\|\partial_\eta \mathbf{u}\|} Q_1 \left(\frac{\|\partial_\xi \mathbf{u}\|}{\|\partial_\eta \mathbf{u}\|} \right) & 0 \end{pmatrix} \mathbf{R}^\top, \quad (69)$$

where \mathbf{R} is the Euclidean normalisation matrix, and the coefficient functions Q_1, Q_2 are those stated in Lemma 5.

Equivariance of the PDE (66) with regard to Euclidean transformations of the u - v plane follows immediately from its derivation for a special case and transfer to the general case by a Euclidean transformation.

Univariate median filtering is contained in the statement of Lemma 5 when v_y is sent to 0. In this case, the first PDE (61) becomes $u_t = u_{yy}$ by virtue of $Q_1(\infty) = 0$, $Q_2(0) = 1$, and the previous remark. This translates to $u_t = u_{\xi\xi}$ in the general setting of Proposition 6, i.e. the (mean) curvature motion equation, thus reproducing exactly the result of [27].

Oja and transformation–retransformation L^1 median. We turn now to the two minimisation-based affine equivariant medians. As was shown in [78], Oja median filtering and transformation–retransformation L^1 median filtering approximate the same PDE, i.e. they are asymptotically equivalent. The following lemma states the PDE limit for Oja median filtering in a normalised geometric setting. Since now affine transformations of the data space can be used for normalisation, a simpler case – with a unit Jacobian – is sufficient to consider in this step.

LEMMA 7 . [78, Lemma 2] For a $(2,2)$ -image \mathbf{u} with a regular point \mathbf{x}_0 where $\mathbf{D}\mathbf{u}(\mathbf{x}_0) = \operatorname{diag}(1, 1)$, the local PDE limit of $(\operatorname{med}_{\text{Oja}}, \mathcal{D})$ -filtering of \mathbf{u} at \mathbf{x}_0 with time scale $\varrho^2/24$ is

$$u_t = u_{xx} + 3u_{yy} - 2v_{xy}, \quad (70)$$

$$v_t = 3v_{xx} + v_{yy} - 2u_{xy}. \quad (71)$$

The setting described can be reached from a generic geometric situation by an affine transform in the data space. It is worth noting that the PDE system (70), (71) coincides exactly with the special case $u_x = v_y = 1$ of Lemma 5 (rewritten to the time scale $\varrho^2/24$ of Lemma 7). Transformation–retransformation L^1 filtering coincides in this case with standard L^1 filtering. Thereby, reverting the affine transform leading to the setting of Lemma 7 yields the general PDE limit not only for Oja but also for transformation–retransformation L^1 filtering. In this context it is important to notice that the covariance matrix of the data within the patch D_ϱ is (up to scaling) asymptotically equal to $\mathbf{D}\mathbf{u}\mathbf{D}\mathbf{u}^\top$ such that the affine transform based in the definition of the continuous transformation–retransformation L^1 median essentially becomes $\mathbf{D}\mathbf{u}^{-1}$, compare [78, Def. 1], where a continuous version of the transformation–retransformation L^1 median is stated using this transform directly.

The general PDE limit result is stated in the following proposition that combines the two results that were stated in [78] separately for the Oja median and the transformation–retransformation L^1 median.

PROPOSITION 8 [78, Theorem 1 and Corollary 1]. For $(2,2)$ -images \mathbf{u} , both $(\operatorname{med}_{\text{Oja}}, \mathcal{D})$ -filtering with the Oja median as aggregator as well as $(\operatorname{med}_{\text{TRL}^1}, \mathcal{D})$ -filtering with the

transformation–retransformation L^1 median as aggregator and the disc family \mathcal{D} as scaled selector have the regular PDE limit with time scale $\tau(\varrho) = \varrho^2/24$ given by

$$\mathbf{u}_t = 2 \Delta \mathbf{u} + \mathbf{A}(\mathbf{D}\mathbf{u})(\mathbf{u}_{yy} - \mathbf{u}_{xx}) + \mathbf{B}(\mathbf{D}\mathbf{u})\mathbf{u}_{xy} \quad (72)$$

with the coefficient matrices

$$\mathbf{A}(\mathbf{D}\mathbf{u}) := \frac{1}{u_x v_y - u_y v_x} \begin{pmatrix} u_x v_y + u_y v_x & -2u_x u_y \\ 2v_x v_y & -u_x v_y - u_y v_x \end{pmatrix}, \quad (73)$$

$$\mathbf{B}(\mathbf{D}\mathbf{u}) := \frac{2}{u_x v_y - u_y v_x} \begin{pmatrix} u_x v_x - u_y v_y & -u_x^2 + u_y^2 \\ v_x^2 - v_y^2 & -u_x v_x + u_y v_y \end{pmatrix}. \quad (74)$$

The derivation of the PDE of Proposition 8 by affine transformation immediately implies its equivariance under affine transformations of the data space. Interestingly, the PDE itself is even equivariant under affine transformations of the x - y plane. Regarding the approximation of multivariate median filtering, however, the Euclidean disc-shaped structuring element allows only for Euclidean transformations of the x - y plane.

To understand the effect of the PDE limit from Proposition 8 as an image evolution, we remark that it consists of three contributions. The first, $\Delta \mathbf{u} + \mathbf{A}(\mathbf{D}\mathbf{u})(\mathbf{u}_{yy} - \mathbf{u}_{xx})$, corresponds to $2u_{yy}$ and $2v_{xx}$ in the equations (70)–(71) of the lemma, and can be understood as independent (mean) curvature motion in the two components u and v , which is in analogy with the evolution (24) approximated by univariate median filtering. The second part, $\Delta \mathbf{u}$, corresponding to $u_{xx} + u_{yy}$ and $v_{xx} + v_{yy}$ in the lemma, is a homogeneous diffusion process that blurs the image, and is not present in the univariate process (24). The third component is the interaction term $\mathbf{B}(\mathbf{D}\mathbf{u})\mathbf{u}_{xy}$ that creates a cross-influence between the u and v components and has obviously no analogue in the univariate case.

Half-space median. The previous results can be extended even to bivariate half-space median filtering.

PROPOSITION 9 [80]. *For a (2, 2)-image \mathbf{u} with a regular point \mathbf{x}_0 where $\mathbf{D}\mathbf{u}(\mathbf{x}_0) = \text{diag}(1, 1)$, the local PDE limit of $(\text{med}_{\text{HS}}, \mathcal{D})$ -filtering of \mathbf{u} at \mathbf{x}_0 with time scale $\varrho^2/24$ is given by (70), (71).*

As a consequence, also the general PDE limit from Proposition 8 carries over to half-space median filtering.

In the light of the equivariance discussion in Section 4.4 this has an interesting implication: The PDE limit (72) is equivariant even under projective transformations of the data space, as long as these do not take the bounded set of image values in the neighbourhood of the regular location under consideration to infinity. This can also be verified directly by applying a projective transformation to (72).

In other words, *although Oja and transformation–retransformation L^1 median filtering are merely affine equivariant, their infinitesimal limit is even projective equivariant.*

Convex-hull-stripping median. No infinitesimal analysis of the convex-hull-stripping median as filter for multivariate images is available so far. Since with the results reported in Section 4.5 the space-continuous process as such can now be described, such an analysis may be achieved in future work. We conjecture that the PDE limit of this process coincides with the one for Oja, transformation–retransformation L^1 and half-space median filtering.

Oja and transformation–retransformation L^1 median filtering with amoeba structuring elements. In the bivariate planar case, also a PDE limit for multivariate amoeba median filtering could be obtained [79]. This result is restricted to Oja and transformation–retransformation L^1 medians; the standard L^1 median case in combination with amoebas appears too complicated for analysis so far.

Unlike for the previous cases, image information now enters not only the aggregation step by the multivariate median but also the computation of the amoeba structuring elements. These influences are decomposed in the analysis in [79]. Whereas the aggregation step by median filtering can again be normalised by affine transformations in the data space, and Lemma 7 for the Oja median together with its counterpart for the transformation–retransformation L^1 median can be reused, the amoeba computation only admits a Euclidean normalisation. The influence of the amoeba structuring elements is described for an appropriate normalised case by the following lemma.

LEMMA 10 . [79, Lemma 2 and Proof of Theorem 2] Consider a $(2, 2)$ -image with domain Ω . Assume that $\mathbf{x}_0 = \mathbf{0} \in \Omega$ is a regular location for \mathbf{u} , and $\mathbf{D}\mathbf{u}(\mathbf{x}) = \text{diag}(1, 1)$ for all $\mathbf{x} \in \Omega$. At $\mathbf{0}$, let an amoeba structuring element $\mathcal{A}(\mathbf{0})$ be given in polar coordinates (r, φ) with $x = r \cos \varphi$, $y = r \sin \varphi$ by its contour $r(\varphi) = \varrho - a(\varphi)$, $a(\varphi) := \frac{1}{2}\varrho^2\beta^2(\alpha_1 \cos^3 \varphi + \alpha_2 \cos^2 \varphi \sin \varphi + \alpha_3 \cos \varphi \sin^2 \varphi + \alpha_4 \sin^3 \varphi)$. Then one step of Oja or transformation–retransformation L^1 median filtering of \mathbf{u} at $\mathbf{0}$ within $\mathcal{A}(\mathbf{0})$ approximates an explicit time step of size $\tau = \varrho^2/24$ of the PDE system

$$u_t = -9\beta^2\alpha_1 - 3\beta^2\alpha_3, \quad v_t = -3\beta^2\alpha_2 - 9\beta^2\alpha_4. \quad (75)$$

Reverting the normalisations and combining the influences of amoeba computation and multivariate median filtering, the general PDE limit as stated in the following proposition is obtained. Due to the Euclidean normalisation for the amoeba computations, the geometric coordinates and Euclidean normalisation matrix appear again in this result.

PROPOSITION 11 [79, Theorems 1 and 2]. For $(2, 2)$ -images \mathbf{u} , both $(\text{med}_{\text{Oja}}, \mathcal{A}_\beta)$ -filtering with the Oja median as aggregator as well as $(\text{med}_{\text{TRL}^1}, \mathcal{A}_\beta)$ -filtering with the transformation–retransformation L^1 median as aggregator and the amoeba family \mathcal{A}_β for given $\beta > 0$ as scaled selector have the regular PDE limit with time scale $\tau(\varrho) = \varrho^2/24$ given by

$$\partial_t \mathbf{u} = \mathbf{T}_1(\mathbf{D}\mathbf{u})\partial_{\eta\eta}\mathbf{u} + \mathbf{T}_2(\mathbf{D}\mathbf{u})\partial_{\xi\xi}\mathbf{u} + \mathbf{T}_3(\mathbf{D}\mathbf{u})\partial_{\eta\xi}\mathbf{u} \quad (76)$$

where $\boldsymbol{\eta}, \boldsymbol{\xi}$ are the geometric coordinates. The coefficient matrices $\mathbf{T}_i(\mathbf{D}\mathbf{u})$ are given by

$$\mathbf{T}_i(\mathbf{D}\mathbf{u}) := \mathbf{R}\boldsymbol{\Theta}_i(\|\partial_{\boldsymbol{\eta}}\mathbf{u}\|, \|\partial_{\boldsymbol{\xi}}\mathbf{u}\|)\mathbf{R}^\top, \quad i = 1, 2, 3, \quad (77)$$

$$\boldsymbol{\Theta}_1(r, s) := \text{diag}(\vartheta_1(r), \vartheta_2(r, s)), \quad (78)$$

$$\boldsymbol{\Theta}_2(r, s) := \text{diag}(\vartheta_2(r, s), \vartheta_1(s)), \quad (79)$$

$$\boldsymbol{\Theta}_3(r, s) := -2 \begin{pmatrix} 0 & \vartheta_3(r, s) \\ \vartheta_3(s, r) & 0 \end{pmatrix}, \quad (80)$$

$$\vartheta_1(z) := \frac{1 - 8\beta^2 z^2}{(1 + \beta^2 z^2)^2}, \quad (81)$$

$$\vartheta_2(w, z) := \frac{3}{(1 + \beta^2 w^2)(1 + \beta^2 z^2)}, \quad (82)$$

$$\vartheta_3(w, z) := \frac{w}{z} \frac{1 + 4\beta^2 z^2}{(1 + \beta^2 w^2)(1 + \beta^2 z^2)}, \quad (83)$$

with the Euclidean normalisation matrix \mathbf{R} .

6.3 Trivariate Volume Images

We continue with the case of trivariate volume images ($\mathbb{R}^3 \rightarrow \mathbb{R}^3$). Again, this case is of limited practical relevance as volume imaging methods often yield univariate images only or, like diffusion-tensor MRI, already higher-dimensional data. Results are available for the Oja and transformation–retransformation L^1 median. In the following, $\mathbf{I} = \text{diag}(1, 1, 1)$ denotes the 3×3 unit matrix.

LEMMA 12 . [78, Lemmas 3 and 4] For a $(3, 3)$ -image \mathbf{u} with a regular point \mathbf{x}_0 where $D\mathbf{u}(\mathbf{x}_0) = \mathbf{I}$, the local PDE limit of $(\text{med}_{\text{Oja}}, \mathcal{B}^3)$ -filtering as well as $(\text{med}_{L^1}, \mathcal{B}^3)$ -filtering of \mathbf{u} at \mathbf{x}_0 with time scale $\varrho^2/20$ is

$$u_t = u_{xx} + 2(u_{yy} + u_{zz}) - (v_{xy} + w_{xz}) \quad (84)$$

$$v_t = v_{yy} + 2(v_{xx} + v_{zz}) - (u_{xy} + w_{yz}) \quad (85)$$

$$w_t = w_{zz} + 2(w_{xx} + w_{yy}) - (u_{xz} + v_{yz}). \quad (86)$$

Again, the general result is obtained by reverting an affine transform that takes a generic regular point to the special situation of the lemma. Similarly as in the bivariate planar case, it is important to notice that the transform by $D\mathbf{u}^{-1}$ also coincides with the asymptotic limit of the covariance-based transform used in the transformation–retransformation L^1 median.

PROPOSITION 13 [78, Theorem 2 and Prop. 2]. For $(3, 3)$ -images \mathbf{u} , $(\text{med}_{\text{Oja}}, \mathcal{B}^3)$ -filtering with the Oja median as aggregator as well as $(\text{med}_{\text{TRL}^1}, \mathcal{B}^3)$ -filtering with the transformation–retransformation L^1 median as aggregator and the ball family \mathcal{B}^3 as scaled selector in both cases have the regular PDE limit with time scale $\tau(\varrho) = \varrho^2/60$ given by

$$\begin{aligned} \mathbf{u}_t = & 5 \Delta \mathbf{u} + \mathbf{A}_1(D\mathbf{u})(\mathbf{u}_{yy} - \mathbf{u}_{xx}) + \mathbf{A}_2(D\mathbf{u})(\mathbf{u}_{zz} - \mathbf{u}_{xx}) \\ & + \mathbf{B}_1(D\mathbf{u})\mathbf{u}_{xy} + \mathbf{B}_2(D\mathbf{u})\mathbf{u}_{xz} + \mathbf{B}_3(D\mathbf{u})\mathbf{u}_{yz} \end{aligned} \quad (87)$$

where for $\mathbf{D} := D\mathbf{u}$ the coefficient matrices are given by

$$\mathbf{A}_1(\mathbf{D}) := \mathbf{I} - 3 \mathbf{D} \text{diag}(0, 1, 0) \mathbf{D}^{-1}, \quad (88)$$

$$\mathbf{A}_2(\mathbf{D}) := \mathbf{I} - 3 \mathbf{D} \text{diag}(0, 0, 1) \mathbf{D}^{-1}, \quad (89)$$

$$\mathbf{B}_1(\mathbf{D}) := -3 \mathbf{D} \begin{pmatrix} 0 & 1 & 0 \\ 1 & 0 & 0 \\ 0 & 0 & 0 \end{pmatrix} \mathbf{D}^{-1}, \quad (90)$$

$$\mathbf{B}_2(\mathbf{D}) := -3 \mathbf{D} \begin{pmatrix} 0 & 0 & 1 \\ 0 & 0 & 0 \\ 1 & 0 & 0 \end{pmatrix} \mathbf{D}^{-1}, \quad (91)$$

$$\mathbf{B}_3(\mathbf{D}) := -3 \mathbf{D} \begin{pmatrix} 0 & 0 & 0 \\ 0 & 0 & 1 \\ 0 & 1 & 0 \end{pmatrix} \mathbf{D}^{-1}. \quad (92)$$

6.4 Trivariate Planar Images

The case of trivariate planar images ($\mathbb{R}^2 \rightarrow \mathbb{R}^3$) is of high practical interest since the vast majority of colour images falls into this category. Asymptotic analysis results are available for Oja and transformation–retransformation L^1 median filtering. A PDE limit stated in [81] for standard L^1 median filtering of n -variate planar images that could be applied to trivariate planar images was incomplete; a corrected result still needs to be published.

Also in the case of trivariate planar images both Oja and transformation–retransformation L^1 median filtering approximate the same PDE as stated in the following results. By $\mathbf{I}^{3,2} = \begin{pmatrix} 1 & 0 \\ 0 & 1 \\ 0 & 0 \end{pmatrix}$ we will abbreviate a “truncated unit matrix”.

LEMMA 14 . [78, Lemma 5 and Remark 12] For a $(2, 3)$ -image \mathbf{u} with a regular point \mathbf{x}_0 where $\mathbf{D}\mathbf{u}(\mathbf{x}_0) = \mathbf{I}^{3,2}$, the local PDE limit of $(\text{med}_{\text{Oja}}, \mathcal{D})$ -filtering as well as of $(\text{med}_{L^1}, \mathcal{D})$ -filtering of \mathbf{u} at \mathbf{x}_0 with time scale $\varrho^2/24$ is

$$u_t = u_{xx} + 3u_{yy} - 2v_{xy} \quad (93)$$

$$v_t = 3v_{xx} + v_{yy} - 2u_{xy} \quad (94)$$

$$w_t = 2w_{xx} + 2w_{yy} . \quad (95)$$

Generic regular points can be transformed to the situation of the lemma using the affine transform \mathbf{D}_3^{-1} where

$$\mathbf{D}_3 := \left(\partial_x \mathbf{u} \mid \partial_y \mathbf{u} \mid \partial_x \mathbf{u} \times \partial_y \mathbf{u} \right) \quad (96)$$

is a rank-three extension of the Jacobian $\mathbf{D}\mathbf{u}$. Again, this transform can be obtained also from the covariance-matrix construction in the transformation–retransformation L^1 median with appropriate handling of the dimensionality issues discussed in Section 5.2, compare also [78, Section 3.3.2].

PROPOSITION 15 [78, Theorem 3 and Prop. 3]. For $(2, 3)$ -images \mathbf{u} , $(\text{med}_{\text{Oja}}, \mathcal{D})$ -filtering with the Oja median as aggregator as well as $(\text{med}_{\text{TRL}^1}, \mathcal{D})$ -filtering with the transformation–retransformation L^1 median as aggregator and the disc family B^2 as scaled selector in both cases have the regular PDE limit with time scale $\tau(\varrho) = \varrho^2/24$ given by

$$\mathbf{u}_t = 2 \Delta \mathbf{u} + \mathbf{A}(\mathbf{D}\mathbf{u})(\mathbf{u}_{yy} - \mathbf{u}_{xx}) + \mathbf{B}(\mathbf{D}\mathbf{u})\mathbf{u}_{xy} \quad (97)$$

where for $\mathbf{D} := \mathbf{D}\mathbf{u} = (\partial_x \mathbf{u} \mid \partial_y \mathbf{u})$ and \mathbf{D}_3 from (96) the coefficient matrices are given by

$$\mathbf{A}(\mathbf{D}) := \mathbf{D}_3 \text{diag}(1, -1, 0) \mathbf{D}_3^{-1} , \quad (98)$$

$$\mathbf{B}(\mathbf{D}) := -2 \mathbf{D}_3 \begin{pmatrix} 0 & 1 & 0 \\ 1 & 0 & 0 \\ 0 & 0 & 0 \end{pmatrix} \mathbf{D}_3^{-1} . \quad (99)$$

Note that \mathbf{D}_3 , the 3×3 matrix obtained by enlarging the 2×3 Jacobian $\mathbf{D}\mathbf{u}$ with a third column orthogonal to the first two ones, is regular if and only if $\mathbf{D}\mathbf{u}$ has rank 2 as required in the hypothesis of the proposition. The transformed variables $\hat{\mathbf{u}} := \mathbf{D}_3^{-1} \mathbf{u}$ have the Jacobian $\mathbf{I}^{3,2}$. Any scaling of the third column of \mathbf{D}_3 is actually irrelevant for the statement and proof of the proposition; it cancels out in the evaluation of (98) and (99). It may, however, affect the scaling of deviations from the PDE that occur for positive structuring element radius ϱ .

7 Summary and Outlook

In this paper, we have reviewed selected median concepts for multivariate data focussing on their applicability to image filtering. To this end, the definitions of multivariate medians have been presented and traced back to different aspects of the univariate median that they generalise, and some important properties, especially regarding equivariance to groups or sets of data transformations, have been discussed. Emphasis has been put on the relation between discrete and continuous modelling since this is a crucial issue in image and shape analysis applications where one is concerned with discrete data arising from the spatial sampling of continuous quantities. PDE approximation results for multivariate image median filters were reported to the extent they are available so far. An interesting outcome is that several affine equivariant multivariate median concepts, despite not coinciding as discrete filters, converge to the same process in an infinitesimal limit, which even features a restricted projective equivariance that some of the discrete concepts do not possess.

We hope that this condensed comparative presentation of multivariate median concepts and image filters with focus on the underlying mathematical constructions and resulting properties paves the way to efficient procedures for shape analysis, for example shape simplification and extraction of shape features or characteristics, and robust filtering of geometric data. In ongoing work, we investigate the suitability of multivariate medians to the processing of geometric and texture data on manifolds.

References

- [1] G. Aloupis, S. Langerman, M. Soss, and G. Toussaint. Algorithms for bivariate medians and a Fermat–Torricelli problem for lines. In *Proc. 13th Canadian Conference on Computational Geometry*, pages 21–24, 2001.
- [2] G. Aloupis, S. Langerman, M. Soss, and G. Toussaint. Algorithms for bivariate medians and a Fermat–Torricelli problem for lines. *Computational Geometry*, 26:69–79, 2003.
- [3] L. Alvarez, F. Guichard, P.-L. Lions, and J.-M. Morel. Axioms and fundamental equations in image processing. *Archive for Rational Mechanics and Analysis*, 123:199–257, 1993.
- [4] L. Alvarez, P.-L. Lions, and J.-M. Morel. Image selective smoothing and edge detection by nonlinear diffusion. II. *SIAM Journal on Numerical Analysis*, 29:845–866, 1992.
- [5] J. Astola, P. Haavisto, and Y. Neuvo. Vector median filters. *Proceedings of the IEEE*, 78(4):678–689, 1990.
- [6] J.-F. Aujol, G. Aubert, L. Blanc-Féraud, and A. Chambolle. Image decomposition into a bounded variation component and an oscillating component. *Journal of Mathematical Imaging and Vision*, 22:71–88, 2005.
- [7] J.-F. Aujol and A. Chambolle. Dual norms and image decomposition models. *International Journal of Computer Vision*, 63(1):85–104, 2005.
- [8] T. L. Austin. An approximation to the point of minimum aggregate distance. *Metron*, 19:10–21, 1959.

- [9] D. Bao, S.-S. Chern, and Z. Shen. *An Introduction to Riemann–Finsler Geometry*, volume 200 of *Graduate Texts in Mathematics*. Springer, New York, 2000.
- [10] V. Barnett. The ordering of multivariate data. *Journal of the Royal Statistical Society A*, 139(3):318–355, 1976.
- [11] A. Beck and S. Sabach. Weiszfeld’s method: Old and new results. *Journal of Optimization Theory and Applications*, 164(1):1–40, 2015.
- [12] M. Blum, R. Floyd, V. Pratt, R. Rivest, and R. Tarjan. Time bounds for selection. *Journal of Computer and System Sciences*, 7:448–461, 1973.
- [13] D. Bremner, D. Chen, J. Iacono, S. Langerman, and P. Morin. Output-sensitive algorithms for Tukey depth and related problems. *Statistics and Computing*, 18:259–266, 2008.
- [14] B. M. Brown. Statistical uses of the spatial median. *Journal of the Royal Statistical Society B*, 45(1):25–30, 1983.
- [15] B. M. Brown and T. P. Hettmansperger. Affine invariant rank methods in the bivariate location model. *Journal of the Royal Statistical Society B*, 49(3):301–310, 1987.
- [16] B. Chakraborty and P. Chaudhuri. On a transformation and re-transformation technique for constructing an affine equivariant multivariate median. *Proceedings of the AMS*, 124(6):2539–2547, 1996.
- [17] T. Chan. An optimal randomized algorithm for maximum Tukey depth. In *SODA ’04. Proceedings of the fifteenth annual ACM-SIAM symposium on Discrete algorithms, Jan. 11–14, 2004*, pages 430–436, New Orleans, Louisiana, USA, 2004. SIAM.
- [18] D. H. Chung and G. Sapiro. On the level lines and geometry of vector-valued images. *IEEE Signal Processing Letters*, 7(9):241–243, 2000.
- [19] U. Clarenz, U. Diewald, and M. Rumpf. Anisotropic geometric diffusion in surface processing. In *Proc. IEEE Conference on Visualization*, pages 397–405, Salt Lake City, 2000.
- [20] U. Clarenz, U. Diewald, and M. Rumpf. Processing textured surfaces via anisotropic geometric diffusion. *IEEE Transactions on Image Processing*, 13(2):248–261, 2004.
- [21] Z. Drezner. A note on the Weber location problem. *Annals of Operation Research*, 40:153–161, 1992.
- [22] R. Dyckerhoff, G. Koshevoy, and K. Mosler. Zonoid data depth: Theory and computation. In A. Prat, editor, *Proceedings in Computational Statistics. 12th Symposium held in Barcelona, Spain*, pages 235–240. Physica-Verlag, Heidelberg, 1996.
- [23] U. Eckhardt. Root images of median filters. *Journal of Mathematical Imaging and Vision*, 19:63–70, 2003.
- [24] L. Galvani. Sulla determinazione del centro di gravita e del centro mediano di una popolazione, con applicazioni alla popolazione italiana censita il 1 dicembre 1921. *Metron*, 11:17–48, 1933.

- [25] C. Gini and L. Galvani. Di talune estensioni dei concetti di media ai caratteri qualitativi. *Metron*, 8:3–209, 1929.
- [26] J. C. Gower. The mediancentre. *Journal of the Royal Statistical Society C*, 23(3):466–470, 1974.
- [27] F. Guichard and J.-M. Morel. Partial differential equations and image iterative filtering. In I. S. Duff and G. A. Watson, editors, *The State of the Art in Numerical Analysis*, number 63 in IMA Conference Series (New Series), pages 525–562. Clarendon Press, Oxford, 1997.
- [28] J. B. S. Haldane. Note on the median on a multivariate distribution. *Biometrika*, 35:414–415, 1948.
- [29] J. F. Hayford. What is the center of an area, or the center of a population? *Journal of the American Statistical Association*, 8(58):47–58, 1902.
- [30] T. P. Hettmansperger and R. H. Randles. A practical affine equivariant multivariate median. *Biometrika*, 89(4):851–860, 2002.
- [31] H. Hotelling. Stability in competition. *The Economic Journal*, 39(153):41–57, 1929.
- [32] D. Jackson. Note on the median of a set of numbers. *Bulletin of the American Mathematical Society*, 27:160–164, 1921.
- [33] A. C. Jalba and J. B. T. M. Roerdink. An efficient morphological active surface model for volumetric image segmentation. In M. H. F. Wilkinson and J. B. T. M. Roerdink, editors, *Mathematical Morphology and Its Application to Signal and Image Processing*, volume 5720 of *Lecture Notes in Computer Science*, pages 193–204. Springer, Berlin, 2009.
- [34] A. Kleefeld, M. Breuß, M. Welk, and B. Burgeth. Adaptive filters for color images: median filtering and its extensions. In A. Trémeau, R. Schettini, and S. Tominaga, editors, *Computational Color Imaging*, volume 9016 of *Lecture Notes in Computer Science*, pages 149–158. Springer, Cham, 2015.
- [35] H. Kuhn. A note on Fermat’s problem. *Mathematical Programming*, 4:98–107, 1973.
- [36] H. Kuhn and R. Kuenne. An efficient algorithm for the numerical solution of the generalized Weber problem in spatial economics. *Journal of Regional Science*, 4:21–34, 1962.
- [37] S. Langerman and W. Steiger. Optimization in arrangements. In H. Alt and M. Habib, editors, *STACS 2003. 20th Annual Symposium on Theoretical Aspects of Computer Science, Berlin, Germany*, volume 2607 of *Lecture Notes in Computer Science*, pages 50–61. Springer, Berlin, 2003.
- [38] R. Lerallut, É. Decenci ere, and F. Meyer. Image processing using morphological amoebas. In C. Ronse, L. Najman, and E. Decenci ere, editors, *Mathematical Morphology: 40 Years On*, volume 30 of *Computational Imaging and Vision*, pages 13–22. Springer, Dordrecht, 2005.
- [39] R. Lerallut, É. Decenci ere, and F. Meyer. Image filtering using morphological amoebas. *Image and Vision Computing*, 25(4):395–404, 2007.

- [40] R. Y. Liu. On a notion of data depth based on random simplices. *The Annals of Statistics*, 18(1):405–414, 1990.
- [41] J. Matoušek. Computing the center of planar point sets. In J. Goodman, R. Pollack, and W. Steiger, editors, *Computational Geometry: Papers from the Special Year*, pages 221–230. AMS, Providence, USA, 1991.
- [42] B. Merriman, J. Bence, and S. Osher. Diffusion generated motion by mean curvature. Technical Report CAM 92-18, Department of Mathematics, University of California, Los Angeles, USA, April 1992.
- [43] P. Milasevic and G. R. Ducharme. Uniqueness of the spatial median. *The Annals of Statistics*, 15(3):1332–1333, 1987.
- [44] J. Nevalainen, D. Larocque, and H. Oja. On the multivariate spatial median for clustered data. *The Canadian Journal of Statistics*, 35(2):215–231, 2007.
- [45] A. Niinimaa, H. Oja, and J. Nyblom. Algorithm AS 277: the Oja bivariate median. *Journal of the Royal Statistical Society C*, 41(3):611–617, 1992.
- [46] H. Oja. Descriptive statistics for multivariate distributions. *Statistics and Probability Letters*, 1:327–332, 1983.
- [47] H. Oja and A. Niinimaa. Asymptotic properties of the generalized median in the case of multivariate normality. *Journal of the Royal Statistical Society B*, 47(2):372–377, 1985.
- [48] S. Osher, A. Solé, and L. Vese. Image decomposition and restoration using total variation minimization and the h^{-1} norm. *Multiscale Modeling and Simulation*, 1(3):349–370, 2003.
- [49] L. Ostresh. Convergence and descent in the Fermat location problem. *Transportation Sciences*, 12:153–164, 1978.
- [50] L. Ostresh. On the convergence of a class of iterative methods for solving the Weber location problem. *Operations Research*, 26:597–609, 1978.
- [51] P. Perona and J. Malik. Scale space and edge detection using anisotropic diffusion. *IEEE Transactions on Pattern Analysis and Machine Intelligence*, 12:629–639, 1990.
- [52] A. Rauh and G. Arce. A fast weighted median algorithm based on Quickselect. In *Proc. 2010 IEEE International Conference on Image Processing*, pages 105–108, Hong Kong, 2010.
- [53] T. Ronkainen, H. Oja, and P. Orponen. Computation of the multivariate Oja median. In R. Dutta, P. Filzmoser, U. Gather, and P. J. Rousseeuw, editors, *Developments in Robust Statistics*, pages 344–359. Physica-Verlag, Heidelberg, 2003.
- [54] P. Rousseeuw and I. Ruts. Algorithm AS 307: Bivariate location depth. *Journal of the Royal Statistical Society C*, 45(4):516–526, 1996.
- [55] P. Rousseeuw and I. Ruts. Constructing the bivariate Tukey median. *Statistica Sinica*, 8:827–839, 1998.

- [56] P. Rousseeuw and I. Ruts. The depth function of a population distribution. *Metrika*, 49:213–244, 1999.
- [57] P. Rousseeuw and A. Struyf. Computing location depth and regression depth in higher dimensions. *Statistics and Computing*, 8:193–203, 1998.
- [58] I. Ruts and P. Rousseeuw. Computing depth contours of bivariate point clouds. *Computational Statistics and Data Analysis*, 23:153–168, 1996.
- [59] G. Sapiro. From active contours to anisotropic diffusion: Connections between two basic PDE’s in image processing. In *Proc. 1996 IEEE International Conference on Image Processing*, volume 1, pages 477–420, Lausanne, Switzerland, September 1996.
- [60] G. Sapiro. *Geometric Partial Differential Equations and Image Analysis*. Cambridge University Press, Cambridge, 2001.
- [61] G. Sapiro and A. Tannenbaum. Affine invariant scale-space. *International Journal of Computer Vision*, 11:25–44, 1993.
- [62] A. H. Seheult, P. J. Diggle, and D. A. Evans. Discussion of paper by V. Barnett. *Journal of the Royal Statistical Society A*, 139(3):351–352, 1976.
- [63] R. Serfling. Equivariance and invariance properties of multivariate quantile and related functions, and the role of standardisation. *Journal of Nonparametric Statistics*, 22(7):915–936, 2010.
- [64] D. R. Seymour. Note on Austin’s “An approximation to the point of minimum aggregate distance”. *Metron*, 28:412–421, 1970.
- [65] C. G. Small. Measures of centrality for multivariate and directional distributions. *Canadian Journal of Statistics*, 15(1):31–39, 1987.
- [66] C. G. Small. A survey of multidimensional medians. *International Statistical Review*, 58(3):263–277, 1990.
- [67] C. Spence and C. Fancourt. An iterative method for vector median filtering. In *Proc. 2007 IEEE International Conference on Image Processing*, volume 5, pages 265–268, 2007.
- [68] A. Struyf, M. Hubert, and P. J. Rousseeuw. Clustering in an object-oriented environment. *Journal of Statistical Software*, 1(4):1–30, 1997.
- [69] J. W. Tukey. *Exploratory Data Analysis*. Addison–Wesley, Menlo Park, 1971.
- [70] J. W. Tukey. Mathematics and the picturing of data. In *Proc. of the International Congress of Mathematics 1974*, pages 523–532, Vancouver, Canada, 1975.
- [71] Y. Vardi and C.-H. Zhang. The multivariate L^1 -median and associated data depth. *Proceedings of the National Academy of Sciences*, 97(4):1423–1426, 2000.
- [72] Y. Vardi and C.-H. Zhang. A modified Weiszfeld algorithm for the Fermat-Weber location problem. *Mathematical Programming A*, 90:559–566, 2001.

- [73] T. Viero, K. Öistämö, and Y. Neuvo. Three-dimensional median-related filters for color image sequence filtering. *IEEE Transactions on Circuits and Systems for Video Technology*, 4(2):129–142, 1994.
- [74] V. S. Vladimirov. *Equations of Mathematical Physics*. Marcel Dekker, New York, 1971.
- [75] W. Walter. *Einführung in die Theorie der Distributionen*. BI Wissenschaftsverlag, Mannheim, 3rd edition, 1994.
- [76] A. Weber. *Über den Standort der Industrien*. Mohr, Tübingen, 1909.
- [77] E. Weiszfeld. Sur le point pour lequel la somme des distances de n points donnés est minimum. *Tôhoku Mathematics Journal*, 43:355–386, 1937.
- [78] M. Welk. Multivariate median filters and partial differential equations. *Journal of Mathematical Imaging and Vision*, 56:320–351, 2016.
- [79] M. Welk. PDE for bivariate amoeba median filtering. In J. Angulo, S. Velasco-Forero, and F. Meyer, editors, *Mathematical Morphology and its Applications to Signal and Image Processing*, volume 10225 of *Lecture Notes in Computer Science*, pages 271–283. Springer, Cham, 2017.
- [80] Welk, M.: Asymptotic analysis of bivariate half-space median filtering. In: P.M. Roth, G. Steinbauer, F. Fraundorfer, M. Brandstötter, R. Perko (eds.) *Proceedings of the Joint Austrian Computer Vision and Robotics Workshop*, pp. 151–156. Verlag der Technischen Universität Graz, Graz (2020)
- [81] M. Welk and M. Breuß. Morphological amoebas and partial differential equations. In P. W. Hawkes, editor, *Advances in Imaging and Electron Physics*, volume 185, pages 139–212. Elsevier Academic Press, 2014.
- [82] M. Welk and M. Breuß. The convex-hull-stripping median approximates affine curvature motion. In M. Burger, J. Lellmann, and J. Modersitzki, editors, *Scale Space and Variational Methods in Computer Vision*, volume 11603 of *Lecture Notes in Computer Science*, pages 199–210. Springer, Cham, 2019.
- [83] M. Welk, M. Breuß, and O. Vogel. Morphological amoebas are self-snakes. *Journal of Mathematical Imaging and Vision*, 39:87–99, 2011.
- [84] M. Welk, C. Feddern, B. Burgeth, and J. Weickert. Median filtering of tensor-valued images. In B. Michaelis and G. Krell, editors, *Pattern Recognition*, volume 2781 of *Lecture Notes in Computer Science*, pages 17–24. Springer, Berlin, 2003.
- [85] M. Welk, J. Weickert, F. Becker, C. Schnörr, C. Feddern, and B. Burgeth. Median and related local filters for tensor-valued images. *Signal Processing*, 87:291–308, 2007.
- [86] W. Yin, D. Goldfarb, and S. Osher. Image cartoon–texture decomposition and feature selection using the total variation regularized L^1 functional. In N. Paragios, O. Faugeras, T. Chan, and C. Schnörr, editors, *Variational and Level Set Methods in Computer Vision*, volume 3752 of *Lecture Notes in Computer Science*, pages 73–84. Springer, Berlin, 2005.